Journal of Sol-Gel Science and Technology
https://doi.org/10.1007/s10971-024-06395-9

ORIGINAL PAPER

Mesoporous silica aerogels for sunflower oil refining and investigation of their adsorption performance

Tülay Merve Soylu[1] · Cem Özel[1,2] · Burcu Karakuzu Ikizler[1] · Ali Can Özarslan[1,2] · Pınar Terzioğlu[3] · Yeliz Basaran Elalmis[1,2] · Sevil Yücel[1,2]

Received: 31 December 2023 / Accepted: 18 April 2024

Abstract

Involving a succession of oil refining stages for edible oil production, a notable constraint lies in the necessity to employ diverse adsorbents at various steps within these processes. This study investigates the synthesis of mesoporous silica aerogels from rice husk ash, comparing their efficacy in physical sunflower oil refining with earth clay (Bentonite) and commercial silica (Trisyl). Tetraethyl orthosilicate (TEOS) impact during aging was analyzed using scanning electron microscopy (SEM), Fourier-transform infrared spectroscopy (FTIR), and N_2 adsorption-desorption analyzer to examine alterations in the structure of silica aerogels. The surface areas of TEOS-doped silica aerogel (TSA) and non-TEOS-doped silica aerogel (NTSA) were 296.18 and 267.06 m²/g. Mesoporous silica aerogels were evaluated for their ability to reduce free fatty acids (FFA), peroxide value (PV), phosphorus, and color pigments in sunflower oil. TSA and NTSA demonstrated significant FFA removal, with TSA at 3 wt.% achieving the highest performance of 32.2%. TSA also effectively reduced PV and phosphorus compared to NTSA, Bentonite and Trisyl, exhibiting performance similar to Bentonite in the bleaching process. TEOS-doped silica aerogels have shown promise as adsorbents for impurity removal in sunflower oil and has emerged as the potential adsorbent that can comprehensively and effectively meet the requirements of many edible oil physical refining applications in a singular step.

Graphical Abstract

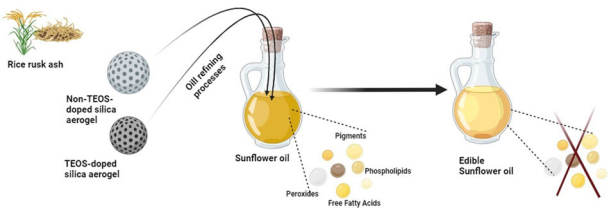

Key words Bleaching · Oil refining · Rice husk ash · Silica aerogel · Sunflower oil · TEOS

Highlights

- Mesoporous silica aerogel synthesis from rice husk ash with/without TEOS-doping.
- Mesoporous silica aerogels were compared to commercial adsorbents.
- For the first time mesoporous silica aerogels were used for oil adsorption with promising results.

✉ Sevil Yücel
syucel@yildiz.edu.tr

[1] Department of Bioengineering, Faculty of Chemical and Metallurgical Engineering, Yildiz Technical University, Esenler, Istanbul, Türkiye

[2] Health Biotechnology Joint Research and Application Center of Excellence, Esenler, Istanbul, Türkiye

[3] Department of Polymer Materials Engineering, Bursa Technical University, Bursa, Türkiye

Published online: 08 May 2024

- TEOS-doped silica aerogel was used to remove acids and peroxide in oil purification effectively.
- TEOS-doped silica aerogel performed effective color and phosphorus removal in oil purification.

1 Introduction

Aerogels are remarkable materials with a porous and lightweight structure in the class of nano/micromaterials. Over recent years, aerogels have gained significant attention due to their exceptional physical, chemical and morphological properties. Aerogels are preferred in many various application areas due to aforementioned properties, for example: filler material for varnishes and paints, catalyst carrier, injection agent, catalyst support adsorbent in the industry [1–4]. One type of aerogel, silica aerogels, consists of cross-linked chains of silicon dioxide (SiO_2) and contains many air-filled pores typically ranging in size from 5 to 100 nanometers [5, 6]. Silica-based adsorbents are widely used for their high physical or chemical adsorption properties, making them a prominent choice in various fields from CO_2 capturing to oil refining [7–9]. Notably, silica aerogels have proven to be efficient adsorbents, exhibiting a capacity for capturing substances like drugs, pollutants, sulfur dioxide, various ions and solvents thanks to the large specific surface area, high pore width and porosity [10–12]. Besides, silica aerogels have also demonstrated effectiveness in adsorbing different heavy metals from water sources [13, 14]. The versatility of silica aerogels makes them valuable materials in environmental remediation, food applications and biomaterial fields as a high promising adsorbent.

Traditional methods for silica aerogel production typically involve the sol-gel process, often followed by the supercritical or ambient drying process. The significant barriers to the widespread commercial production of silica aerogels include their considerable high cost and presence of hazardous materials of the precursors [15–17]. In recent years, there has been a growing trend to replace expensive organoalkoxysilanes like tetramethoxysilane (TMOS) and tetraethoxysilane (TEOS) with more cost-effective alternatives such as bamboo leaf [18], incineration bottom ash [19], fly ash [20], sugarcane bagasse ash [21], and rice husk ash [22–24] in the source of silica and production of silica aerogels. Agricultural waste materials, including rice husk (RH) and rice husk ash (RHA), stand out as a highly promising source of silica. They present fewer toxic precursors and have the potential to lower the cost challenges associated with silica aerogel production, owing to their abundant availability [25–28]. Following the data provided by the United States Department of Agriculture (USDA), global rice production in 2023 is projected to reach an estimated volume of 518.14 million metric tons [29]. Paralleling this increase in rice production, the presence of excess RH and RHA is increasing, stemming from inadequate valorization practices. Besides, this increase in the presence of RHA, accompanied by the limited exploitation of these materials, engenders a spectrum of environmental concerns. In recent days, substantial endeavors have been directed towards enhancing the production of silica aerogels, with RHA assuming a progressively pivotal role within the framework of the "from waste to wealth" paradigm [30–34]. Therefore, silica aerogels were produced from RH or RHA, providing both a cost-effective precursor and a material that is environmentally friendly as well as the use of agricultural waste [35, 36].

A sequence of refining steps (stages) is commonly undertaken within the area of edible oil production. These stages generally contain degumming, neutralization, bleaching, and deodorization [37–39]. Throughout these refining processes, removing unwanted impurities due to a different manufacturing process or a change in vendor for cost reasons is an important objective. Specifically, these impurities include free fatty acids (FFA), phospholipids, heavy metals, color pigments, and peroxides [37]. The efficacy of impurity removal is discernible across multiple stages of the extraction process: phospholipids and trace metals are specifically targeted during the extraction of sticky (wax) substances; FFA and phospholipids are effectively managed during the neutralization phase; decolorization procedures focus on eliminating color substances and soap phases; and the deodorization step serves to eradicate malodorous compounds, including aldehydes, ketones, FFAs, and polyaromatic hydrocarbons, thereby mitigating undesirable odors associated with the oil [40–43]. Researchers commonly employ refining processes to enhance the nutritional quality of various crude oils. Numerous studies have tried to solve the removal of FFAs and other impurities using different adsorbent materials, including activated carbon, calcified zeolite, clay diatomite, and polymeric composites [44–47]. In physical oil refining processes, not only FFA or other impurities have to be removed but also color removal by other materials. Earth or clays (such as Bentonite) facilitate the removal of color from oils in the bleaching step [37, 48, 49]. Furthermore, certain oil manufacturers employ a combination of Bentonite clay and Trisyl®, a commercially available synthetic amorphous micronized silica product, in varying ratios during the physical refining process due to that Trisyl is particularly valued for its ability to selectively remove polar compounds, often associated with undesirable colors and flavors, from vegetable oils and biodiesel feedstocks [50–53]. Indeed, various literature studies have searched the adsorption capacities of specific adsorbents concerning components like FFA, polar substances, and color

pigments found in crude oils [54–58]. However, conventional adsorbents for removing problematic ingredients from oils often face some limitations. Some adsorbents struggle with achieving complete removal, and may unintentionally eliminate beneficial minor components that contribute to flavor, taste, and health benefits [59, 60]. This highlights the need for new adsorbents that selectively target these problematic impurities.

Among the techniques available for removing impurities in vegetable oil, adsorption processes utilizing porous materials have become particularly common. These methods use the porosity features of the materials to extract and separate targeted components. The discovery and development of mesoporous silica has one of the play pivotal role the field of porous materials. Mesoporous silica aerogels offers higher surface area and pore volume compared to some traditional adsorbents, making it particularly well-suited for various applications, with adsorption being a prominent example [44]. The efficacy of mesoporous silica in adsorption applications can be influenced by pore size, as the interactions between mesoporous silica and ingredients may be vary accordingly. Previous research has explored various adsorbents for FFA removal from crude oil, including C18 silica [61], mesoporous silica [62], aminopropyl-modified silica [63], polydimethylsiloxane (PDMS) [64], and magnetic amino-modified silica [65]. However, these materials present certain limitations. Some may involve the use of potentially toxic precursors during synthesis or the precursors for conventional silica synthesis can be expensive [66]. As an alternative to all these, RH and RHAs, characterized by their affordability, non-toxic nature, and status as agricultural waste, hold significant promise as relatively porous materials with high adsorbent and decolorization capacities for crude oils. Interestingly, RH and RHA itself exhibit remarkable adsorption capabilities, which may be attributed in particular to their porous structure. However, their adsorption performance is believed to stem from their varying composition and silica content [67]. In recent study conducted by Schneider et al. the effects of RH and activated carbon in pretreating waste cooking oil to removing of FFA were investigated. The findings indicated that utilizing RH as an adsorbent material for treating waste cooking oil presents a viable alternative for cost reduction in the process. This was attributed to the presence of silanol and hydroxyl groups on the surface of RH, which serve as active sites for adsorption and facilitate the efficient removal of FFA in shorter durations [68]. Recent research by Zainal et al. demonstrated that calcium silicate derived from RHA can serve as an efficient adsorbent for the recovery of FFA from waste frying oil. Also, they found that increasing silica content and achieving higher surface area enhances FFA adsorption capacity in waste frying oil [67].

However, these studies have mostly focused only on a single step in oil refining (FFA removal), whereas phospholipid and color removal performances were not studied and remain largely unexplored. The multifaceted nature of edible oil refining, with its varied impurities, has to present ongoing research to develop potential single adsorbent that can comprehensively and effectively meet these requirements of all physical refining steps (FFA, peroxide, phosphorus and color removing) needs. Moreover, these adsorbents should aim to streamline the oil refining process by minimizing steps, thereby enhancing overall efficiency, and reducing costs by using agricultural wastes as silica source. Silica aerogel is recognized for its exceptional properties, including its high surface area, porosity, and low density, making it highly versatile across various fields. This study investigates a novel application of mesoporous silica aerogel from RHA thanks to its high adsorption capacity in edible oil refining, an innovative approach not previously documented in the literature, thus representing a pioneering contribution to the field. Using silica aerogels brings a new approach and material to physical vegetable oil refining processes and can improve efficiency and effectiveness compared to traditional adsorbents. Utilizing silica aerogel may open up new possibilities and avenues for enhancing the performance of physical oil refining procedures. In this research, a sodium silicate solution derived from RHA served as the silica source, used as a precursor for synthesizing TEOS-doped and non-TEOS-doped mesoporous silica aerogels through the sol-gel methodology. Comprehensive characterizations of the morphology, chemical structure, and textural properties of the produced silica aerogels were carried out employing Scanning Electron Microscopy (SEM)-Energy Dispersive X-ray (EDS), Fourier Transform Infrared (FTIR) and N_2 adsorption-desorption analyzer. Subsequently, the various physical oil refining processes of these silica aerogels were assessed by their application in the purification of sunflower oil, and their performance was compared with commercial adsorbents, Trsiyl and Bentonite. This approach envisages exploiting the sustainable use of environmentally friendly RHA as a feedstock and using mesoporous silica aerogels with unique properties to refine crude oil for achieving edible oil.

2 Materials and Methods

2.1 Materials

RHA was purchased from local company Sınmazlar Foods Inc. (Edirne, Türkiye). Tetraethoxysilane (TEOS, 99%), hydrochloric acid (HCl, 37%), sodium hydroxide (NaOH, 99.9%), nitric acid (HNO_3, 65%), ethanol (99%), and

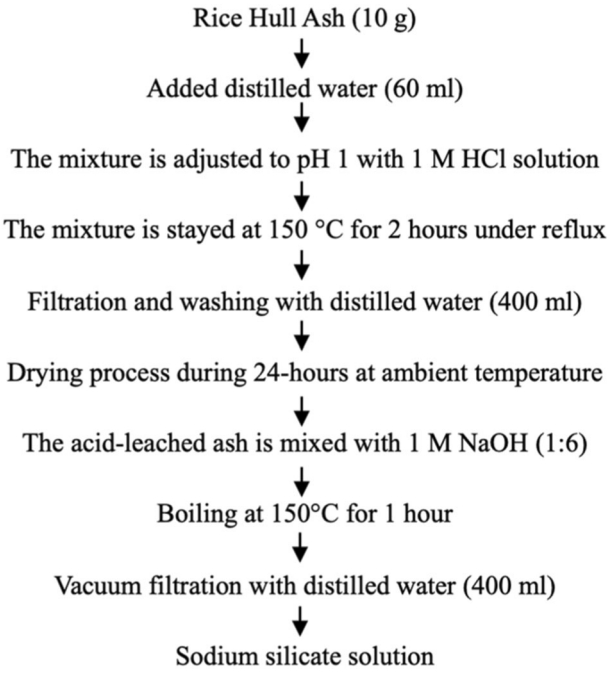

Fig. 1 Flow diagram of the procedure of sodium silicate production solution from RHA

sodium nitrate ($NaNO_3$, 99%) were supplied from Merck (Darmstadt, Germany). N-heptane (99%) was purchased from Sigma Aldrich (St. Louis, MO, USA). Trisyl® 300 (a commercial synthetic silica) was obtained from Grace Davison (Baltimore, MD, USA). Calcium Bentonite was obtained from Amcol Mineral Mining Co. (Edirne, Türkiye). Sunflower oil (*Helianthus annuus*) was provided by Unilever Margarine Inc. (Tekirdağ, Türkiye). The neutralized oil used in the experiments was the oil obtained from the facility after the alkali refining process. All chemicals were employed in their as-received states without further modification. Distilled water used throughout the experiments, was obtained via a water distillation unit (Gesellschaft für Labortechnik mbH, GFL 2002, Germany).

2.2 Production of Sodium Silicate solution

The sodium silicate solution (Na_2SiO_3) was obtained using the alkaline extraction method described in previous studies as illustrated in Fig. 1 [69, 70]. Firstly, RHA was burned in an incineration furnace (Protherm, PLF115M, Türkiye) at 600 °C for 5 h. The 10 g incinerated RHA was weighed and distilled water was added to it in a ratio of 6:1 by weight (incinerated RHA:distilled water=1:6). The RHA-distilled water mixture was adjusted to pH 1 with 1 M HCl solution. A method involving treatment with 1 M HCl (acid leaching) was carried out at 150 °C for 2 h under reflux to eliminate metallic ion contaminants. Subsequently, the acid-leached ash was acquired through filtration and washing of the mixture with 400 ml of distilled water under vacuum, followed by a 24 h drying period at ambient temperature. For alkaline extraction, the acid-leached ash was mixed with 1 M NaOH at a weight ratio of 1:6 (acid-leached ash: 1 M NaOH=1:6), and the mixture was subsequently boiled at 150 °C for 1 h to extract silica. The latest mixture was subjected to vacuum filtration using 400 ml of distilled water, obtaining a sodium silicate solution as a silica source.

2.3 Production of the RHA-based silica aerogels

TEOS-doped (TSA) and non-TEOS-doped (NTSA) RHA-based silica aerogels were produced by modification of the methodology described in our previous study as illustrated in Fig. 2 [70]. In order to obtain silica aqua gel, the pH level of the sodium silicate solution (50 ml) was decreased to 7 by utilizing 1 M HNO_3. These formed gels were subsequently allowed to undergo an aging process at room temperature for 24 h to obtain a more robust silica network. The aged gels were washed three times with distilled water by centrifugation to eliminate formed sodium salts (such as $NaNO_3$) during the condensation reaction. The water in silica aqua gel was replaced by a prepared solution of 80% (v/v) ethanol and 20% (v/v) H_2O and maintained at room temperature for 24 h. Following that, in the preparation of TEOS-doped silica aerogel (TSA), an additional aging process was conducted. This process involved treating the gel with a 70% (v/v) TEOS in ethanol solution for 18 h at room temperature, followed by an additional 4 h at 70 °C. Subsequently, during the solvent exchange step, the gel in 70% (v/v) TEOS–ethanol solution and the gel in 80% (v/v) ethanol solution were washed with n-heptane (100 ml) three times. The gels were kept in 100 ml of n-heptane for 24 h at room temperature. On the following day, the n-heptane was replaced with fresh n-heptane two times, and the gels were centrifugated by centurion scientific centrifuge at 4800 rpm (Andreas Hettich, D72 Germany) and subsequently, gels were dried in an air-dryer (Elektromag, M420P, Türkiye) in 18 h intervals at 50 °C [70].

2.4 Characterization of mesoporous silica aerogels and other adsorbents

FTIR spectra were acquired for all samples at spectral range of 4000–650 cm^{-1} (Shimadzu Corporation, IRPrestige-21, Japan), utilizing an Attenuated Total Reflectance (ATR) at 20 °C to determine functional groups of the material. A total of 15 scans were executed, each at a resolution of 2 cm^{-1} for all samples. The spectra were collected in transmittance mode (T%).

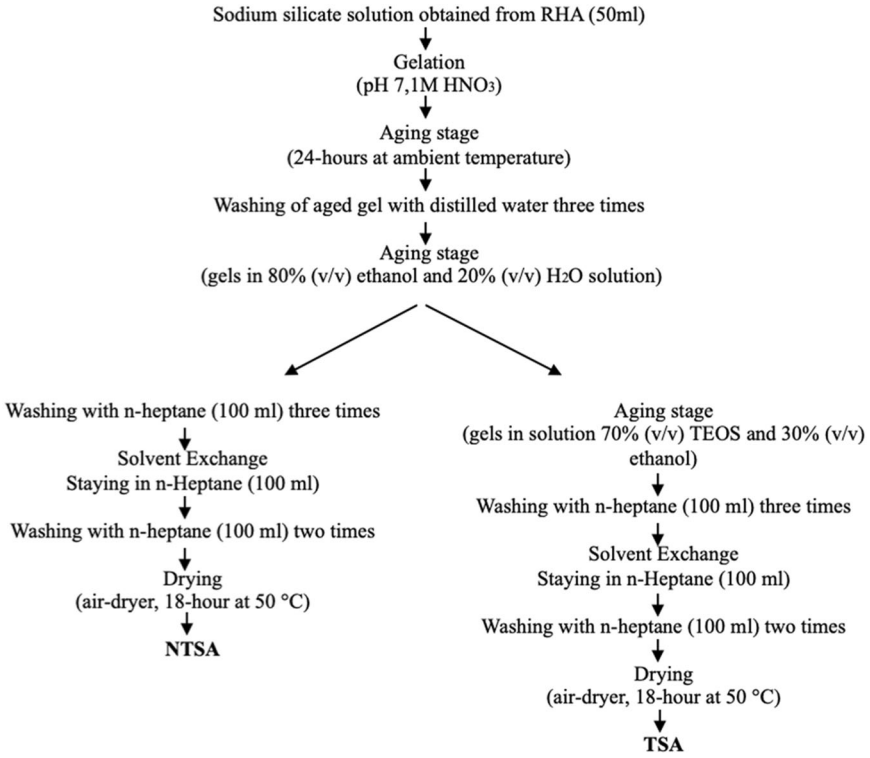

Fig. 2 Flow diagram of TEOS-doped (TSA) and non-TEOS-doped (NTSA) silica aerogels production

SEM analysis was performed using an SEM device (SEM; Zeiss, EVO® Ls 10 T) with an Energy-Dispersive X-ray Spectroscopy apparatus (EDS; Carl Zeiss, SmartEDX) to determine the morphological properties and semi-quantitative elemental compositions of the RHA-based mesoporous silica aerogels, respectively. Before analysis, the samples were coated with a thin layer of gold-palladium using a sputter coater device (Emitech K550X, UK) under vacuum conditions, employing an approximate voltage of 1 kV for 10 min. Micrographs of the aerogels were subsequently captured utilizing varying magnifications.

The textural characteristics of all samples, specific surface area (m^2/g) and pore diameter (Å), which can exhibit variability contingent upon production conditions, were analyzed via utilization of nitrogen (N_2) adsorption-desorption device (TriStar™ II 3020, Micromeritics, USA). High-purity nitrogen (99.999%, Habaş, Türkiye) was employed during the characterization process. Before N_2 adsorption-desorption analysis, the samples were subjected to a degassing procedure facilitated by a continuous N_2 gas flow; samples were to temperatures of 90 °C for 1 h, followed by an elevated temperature of 250 °C for 2 h. To determine specific surface area, the Brunauer-Emmett-Teller (BET) method was employed, a widely acknowledged approach in surface area calculations. Barrett–Joyner–Halenda (BJH) adsorption method was used to determine cumulative pore volume and average pore width.

2.5 Adsorbent treatment and characteristic analysis of the sunflower oil

Crude or neutralized oil (sunflower oil) was weighed into 50 ml flasks. The samples are placed within a shaking water bath (GFL 1086, Germany) maintained at 25 or 90 °C for 20 min. At the end of 20 min, Trisyl, Bentonite, and produced mesoporous silica aerogels or combinations of these adsorbents with Bentonite (Bentonite: other adsorbents 3:1 wt.%) were added in specific ratios (1, 2, and 3 wt. %). The mixture of samples was carefully agitated within a stirred water bath at a constant temperature of 90 °C and a rotational speed of 185 min^{-1}, sustaining this agitation for 30 min. After this mixing, the samples were extracted from the stirred water bath and subjected to centrifugation at 4800 rpm for 30 min. The oil layer remaining on top is removed with the help of a Pasteur pipette and weighed in sample bottles, and the amount of oil remaining after adsorption is noted. This assessment determines the weight of oil remaining post-adsorption by the introduced adsorbents. Within this framework, after performing adsorption studies involving Trisyl, Bentonite, and mesoporous silica aerogels and combinations, a meticulous evaluation was carried out concerning their interaction with crude sunflower oil. This evaluation encompassed the assessment of FFA levels, performances in terms of decolorization and removing peroxides and phospholipids, and the extent of neutral oil losses evident in the resultant oils acquired through the process.

2.5.1 Determination of FFA value

The quantification of FFA was conducted by employing the titration method as proposed in the American Oil Chemists' Society (AOCS) Ca 5a-40 methodology [71]. A certain amount of oil (2 g) was precisely weighed and subsequently dissolved within a solvent composed of diethyl ether and ethanol (25 ml, ratio of 1:1 v/v). After dissolution, 1% phenolphthalein indicator solution was added to the mixture. Titration performed by employing a standardized 0.1 M NaOH solution. An analogous procedure was conducted for a control experiment wherein oil was absent, establishing a baseline comparison. The quantification of FFA content was determined using the formula outlined in Eq. 1 [72, 73]. Equation 2 was employed to calculate the percentage reduction in FFA, utilizing the FFA values of the untreated samples (blank) and the samples post-treatment [68]. This calculation was predicated on the sample's equivalent of oleic acid content.

$$\text{FFA as oleic acid(mg KOH/g)} = \frac{\text{alkali volume (mL)} \times \text{alkali normality} \times 28.2}{\text{sample weight (g)}} \tag{1}$$

$$\text{FFA as oleic acid}(\%) = \left(\frac{FFA_{initial} - FFA_{final}}{FFA_{initial}}\right) \times 100 \tag{2}$$

Where %FFA Reduction percentage; $FFA_{initial}$ acid value of sample without treatment (blank) (mg KOH/g); FFA_{final} acid value of sample after treatment mg KOH/g.

2.5.2 Determination of Peroxide Value (PV)

PV was determined according to AOCS Cd 8-53 [74]. Briefly, 20 ml of chloroform was added to 1 g of oil sample, and 50 ml of acetic acid:chloroform (3:2, v/v) solution was added and shaken until the lipid was completely dissolved. After dissolving the oil, 1 ml of saturated potassium iodide was added and kept in a dark place for 30 min after shaking for 20 s. Then 150 ml of distilled water was added (the oil solvent and water in the titration mixture was 1:3 v/v), followed by 4–5 drops of 1% starch solution and titrated with 0.002 M sodium thiosulfate until a clear color was obtained. The same was done for the blank without oil. The quantification of PV was performed by Eq. 3.

$$\text{PV(mEq/kg)} = \frac{(\text{Vs} - \text{Vb})\text{x N x1000}}{\text{W}} \tag{3}$$

V_b represents the volume (in ml) of sodium thiosulfate solution used for the blank experiment, V_s represents the volume (in ml) of sodium thiosulfate solution used for the sample, N represents the normality of the sodium thiosulfate solution (0.002 M), W corresponds to the weight of the oil sample (1 g).

2.5.3 Color determination

Color analysis for oil before and after adsorption were performed with a Lovibond tintometer, employing cuvettes of varying dimensions in the present study. Specifically, cuvettes measuring ½ inch (12.7 mm) and 5½ inch (133.4 mm) were utilized, with the conversion ratio being 1 inch (25.4 mm). Lovibond tintometer has applicable standards such as AOCS Cc 13e-92, and AOCS Cc 13j-97 [75–77]. Our Lovibond device (PFXi880L; Lovibond, UK) has a color scale range (0–70 Red, 0–70 Yellow, 0–30 Blue, 0–3 Neutral). Our Lovibond device uses the Lovibond® RYBN Color scale. The AOCS-Tintometer® Color Scale is a special red and yellow version of the Lovibond RYBN scale using the AOCS-Tintometer Red Scale.

2.5.4 Phosphorus analysis

Total phosphorus content, which indicates phospholipids content in crude sunflower oil after adsorption, was determined through a modified approach based on the methodology in the study by Shariff et al. [78]. 1 g of oil samples was weighed and after the addition of winterized oil, phosphorus values were measured. Phosphorus value was determined using an atomic absorption spectrophotometer (PerkinElmer, AAnalyst™ 700, Shelton, CT, USA) after adsorption process.

2.5.5 Total oil loss

Although effective in eliminating specific impurities from oils, the adsorption process is accompanied by an inevitable occurrence of neutral oil loss. To ascertain the extent of neutral oil loss, a comparative assessment was conducted by measuring the oils' weights prior to and subsequent to the adsorption procedure. The neutral oil loss was subsequently deduced by calculating the disparity between these two measurements by Eq. 4.

$$\text{Total Oil Loss}\,(\%) = \frac{(A_e - A_f)}{\text{W}}\text{x100} \tag{4}$$

Where W denotes total amount of oil before refining (g), A_f signifies adsorbent amount before refining (g) and A_e represents adsorbent amount after refining (g).

2.6 Statistical analysis

All statistical analyses were performed using one-way analysis of variance (ANOVA) with OriginPro Version 2024 (OriginLab Corporation, Northampton, MA, USA). Data are presented as mean ± standard deviation (SD). Statistical differences between groups were assessed using one-way ANOVA or Tukey's multiple comparison test. In all cases, a *p*-value of less than 0.05 was considered statistically significant.

3 Result and discussion

3.1 FTIR analysis

FTIR results provide insights into the functional groups of silica aerogels and other adsorbent structures. This information is crucial for determining the chemical properties of adsorbents [79, 80]. FTIR spectra of silica aerogels and other adsorbent samples are depicted in Fig. 3. The primary peaks for silica-based materials were detected in the wavenumber range of 720–850, 930–960, and 1000–1140 cm^{-1}, exhibiting similarity across all analyzed samples of adsorbents. The robust peak identified in the wavenumber range of 720–850 cm^{-1} was caused by the Si–O–Si symmetric stretching (Si–O(s) s.s.) and was consistently observed in all adsorbents [81–83]. Besides, the peak identified in the 930–960 cm^{-1} wavenumber range can be indicating attributed to the in-plane stretching vibrations of Si–O(s) in the SiO_4 tetrahedron or the presence of Si–OH [5, 82, 84, 85]. The strong peak observed within the wavenumber range of 1000–1140 cm^{-1} in both aerogels serves as an indicative marker for the presence of Si–O–Si (siloxane) groups within the silica network, strongly implies the formation of these bonds through a condensation reaction. These peaks are associated explicitly with the asymmetric stretching (Si–O(s) a. s.) of siloxane, providing valuable insights into the structural composition of the adsorbents [81, 82, 86]. Specifically, the condensation reaction involves the interaction between Si–OH and Si–O–C_2H_5 groups. This information provides robust evidence regarding the formation mechanism of the silica network structure within both silica aerogels. Besides, the discernible peaks at approximately 1360 and 1440 cm^{-1} in the RHA indicate CH groups (C–H asymmetric and symmetric deformation of –CH_3 and –CH_2 groups) arising from the organic constituents within the RHA structure [82, 87–90]. Significantly, the absence of these peaks in the spectra of the TSA and NSA samples derived from RHA can also serve as evidence of the successful production of both aerogels [82]. The findings collectively indicate the similar peaks and successful synthesis of both silica aerogels.

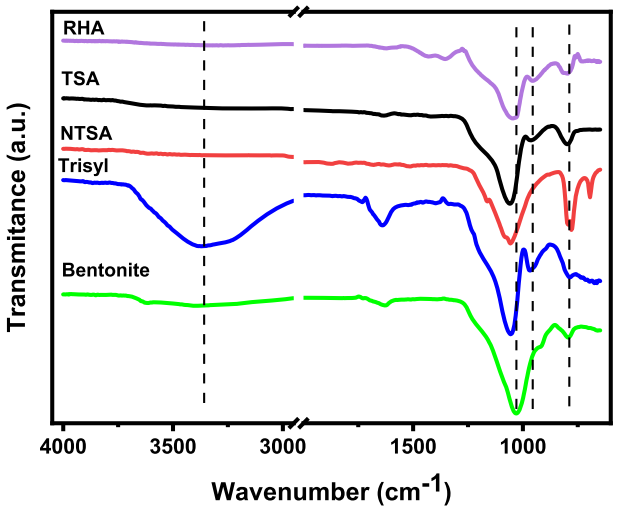

Fig. 3 FTIR spectra of RHA and adsorbent samples

The presence of characteristic peaks observed in silica aerogels was also discerned in the Bentonite and Trisyl samples, proving a similarity in structural features among these materials. The Bentonite samples exhibit distinctive peaks at 1650 and 910 cm^{-1} wavenumber alongside other peaks; these particular peaks can be indicative of bending –OH (adsorbed water) and bending Al–Al–OH, providing insights into the molecular structure of the Bentonite [91, 92]. Besides, a wide-ranging peak of Trisyl extending from 3000 to 3700 cm^{-1} is observed. This peak can be indicative of the O–H stretching vibration peak associated with hydrogen-bonded water (H–O–H$^{\cdots}$H) and the Si–OH stretching of surface silanols hydrogen-bonded to molecular water (Si–OH$^{\cdots}$ H–O–H) [82, 93]. The observed higher this peak for Trisyl compared to other adsorbents might be attributed to its high specific surface area [94]. Also, the weak peak in the wavenumber range of 1700–1600 cm^{-1} in Trisyl is due to deformation vibrations caused by physically adsorbed water on its surface [82].

3.2 SEM-EDS Analysis

The SEM micrographs in Fig. 4a, b reveal the surface texture and morphological characteristics of the synthesized silica aerogels. Figure 4a, b shows the irregular shape of the

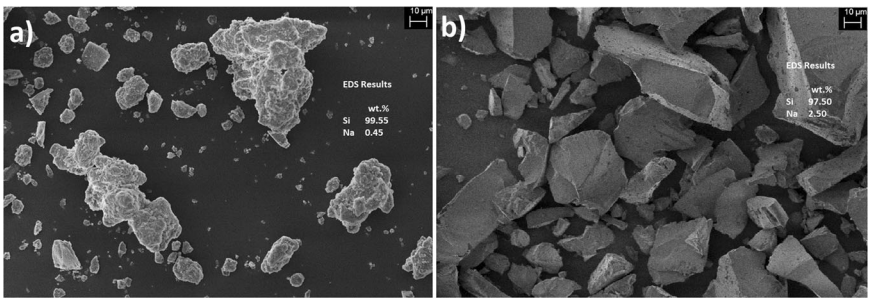

Fig. 4 SEM images of (**a**) TSA and (**b**) NTSA (scale bar is 10 µm). Insets show the EDS analysis of silica aerogels

silica aerogel samples, showcasing a heterogeneous distribution in particle size. Noteworthy is the observation that the measured particle sizes of the prepared TSA samples range between 50 and 90 nm, as predicted. Furthermore, introducing TEOS doping in TSA led to a heightened cluster density and a robust gel framework.

Consequently, the TSA gel network demonstrated increased resilience against capillary pressure during the drying process at ambient pressure, effectively minimizing the formation of cracks compared to NTSA. This enhancement in structural integrity can suggest that TEOS doping contributes to the overall stability of the aerogel, making it more resistant to the stresses induced by the drying process [95]. The particles present a rough surface, which is attributed to the presence of abundant voids, and TSA exhibits tendencies toward agglomeration, as depicted in Fig. 4a.

EDS was applied to analyze the elemental composition of the TSA and NTSA, contributing to an investigation of their chemical constituents. The confirmation of silica aerogel formation is also substantiated by the conspicuous presence of silicon (Si) in the EDS results [96]. The EDS analysis reveals that the TSA and NTSA composition comprises 99.55 Si, 0.45 wt. % Na and 97.50% Si, 2.50 wt. % Na, as depicted in Fig. 2a, b insets, respectively. These elemental percentages align closely with the expected composition of silica aerogels from RHA, providing evidence of the successful synthesis of both aerogels [69]. The EDS results, indicating a relatively low percentage of sodium (Na, 0.50 wt.%), suggest that Na^+ ions present in the TSA content are likely to undergo partial removal from the pores of the silica network during the solvent exchange process of the silica aerogels [97]. This observation may have resulted from the dynamic nature of the aerogel synthesis, where certain components, such as Na^+ ions, may be subject to extraction or displacement as part of the post-synthesis treatments.

3.3 N_2 Adsorption-Desorption Analysis

The specific surface area and porosity characteristics of the adsorbents were determined through nitrogen adsorption/desorption isotherm analysis by surface area and pore size analyzer. The BET method determined the surface area, while the pore size distribution and pore volume values were ascertained using the BJH method. The outcomes for specific surface area, pore size, and pore volume of the adsorbents, along with their respective adsorption/desorption isotherms, are presented in Table 1 and Fig. 5, respectively. Consistent with earlier studies, the N_2 adsorption/desorption results indicate that the TSA and NTSA, along with other adsorbent powders, exhibit a high specific BET surface area and BJH pore volume [4, 70]. The

Table 1 Textural properties of the different adsorbents

Sample	S_{BET} (m2/g)	BJH pore size (nm)	BJH Pore Volume ($cm^3\ g^{-1}$)
TSA	296.18 ± 3.05	8.710	0.756
NTSA	267.06 ± 1.78	6.483	0.211
Trisyl	632.43 ± 3.43	7.548	1.070
Bentonite	167.96 ± 1.52	5.428	0.205

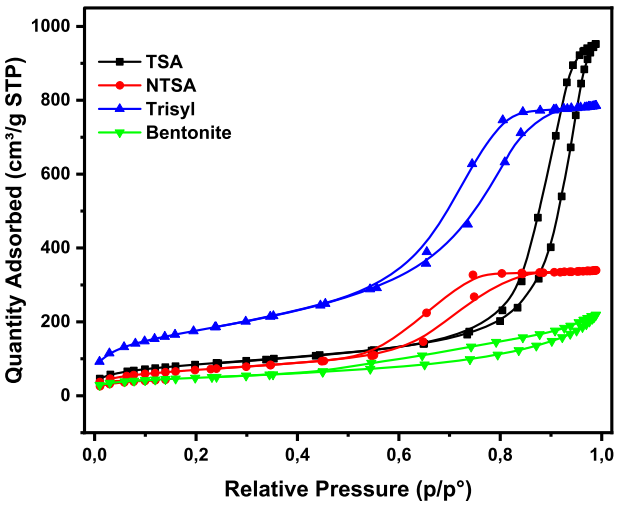

Fig. 5 N_2 adsorption/desorption isotherms of the different adsorbents. N_2 adsorption/desorption data were calculated by the BET method

specific BET surface areas for the TSA, NTSA, Trisyl, and Bentonite are 296.18 ± 3.05, 267.06 ± 1.78, 632.43 ± 3.43, and 167.96 ± 1.52 m^2/g respectively. Adsorbents have been observed at 8.710, 6.483, 7.548, and 5.428 nm average pore diameter and 0.756, 0.211, 1.070 and 0.2048 $cm^3\ g^{-1}$ total pore volume, respectively.

The doping of TEOS leads to an increase in the specific surface area, pore diameter, and volume of the silica aerogel sample. These results can be attributed to the reinforcement of the gel structure caused by the incorporation of TEOS into the silica sol. Besides, the addition of TEOS might impede the occurrence of cracking in the gel, strengthening its overall structure. In contrast, in the absence of TEOS, capillary tension induces shrinkage in the silica gel network, resulting in gel cracking and decreasing the pore size and specific surface area [70]. The study conducted by Tadjarodi et al. involved the synthesis of silica aerogel from RHA, followed by drying under atmospheric pressure [98]. Their observations revealed that adding TEOS increased the specific BET surface area from 220 to 315 m^2/g and expanded the pore size from 8.3 to 9.8 nm. The findings from the present study align with and corroborate the outcomes reported in this study. As investigated in this study, Ca Bentonite adsorbent demonstrated similar to other types of Bentonites, with relatively lower surface area and pore

size results due to inherent structural characteristics of Ca Bentonite [99, 100]. Furthermore, the findings derived from using Trisyl in the present study exhibit a marked resemblance to the outcomes results in previously published research featuring Trisyl300B adsorbent [101, 102]. In strict accordance with the classification standards set forth by the International Union of Pure and Applied Chemistry (IUPAC), the demarcation of pore sizes is systematically structured into three distinctive categories: macrospores (>50 nm), mesopores (2–50 nm), and microspores (<2 nm), respectively [103]. The deduction that can be drawn from the results is that all the adsorbents under consideration exhibit a mesoporous structure. These results highlight all adsorbent materials' high porosity and surface area characteristics, including our synthesized silica aerogels. They show their potential utility in oil adsorption applications due to their high adsorption capacity.

Figure 5 shows the N_2 adsorption–desorption isotherms of aerogel samples. The geometrical characteristics of the hysteresis loop in the N_2 adsorption-desorption isotherms indicate the present pore structure and shape within the material [104]. TSA, NTSA aerogels, and Trisyl confirm a type IVa isotherm, aligning with the typical features of mesoporous materials. Furthermore, Bentonite can be characterized as exhibiting a type IVa isotherm [105]. These observations are consistent with the IUPAC classification for mesoporous materials for adsorbents [106]. Moreover, the desorption cycles of these samples represented a hysteresis loop attributed to capillary condensation, a characteristic phenomenon observed in mesoporous materials [107].

The TSA sample displayed an H1-type hysteresis loop, indicating cylindrical pores open at both ends and well-defined cylindrical-shaped pore structures. Conversely, NTSA exhibited an H2-type hysteresis, characteristic of "inkbottle" pores. The different hysteresis loops observed for the TSA and NTSA samples confirm that TEOS doping impacted pore shape. This finding underscores the influence of TEOS doping on specific surface area and the pore shape of the aerogel samples. The agreement of these results with our previous study suggests a consistent pattern in the influence of TEOS doping on pore properties [70]. Hysteresis loops of the TSA and Trisyl samples were similar, H1-type hysteresis loops. The hysteresis loop characteristics exhibited by Bentonite align with the H4-type hysteresis, typically associated with samples containing mono-multilayer adsorption on narrow slit-shaped pores found among plate-like particles. This specific type of hysteresis strongly indicates the presence of layered clay materials, such as Bentonite, characterized by complex interiors featuring non-uniform micropores and mesopores. The observed adsorption/desorption profiles further confirm Bentonite's intricate and layered structure, providing valuable insights into its pore morphology and adsorption behavior [108, 109]. The different textural properties observed among the adsorbents provide the distinct characteristics of each material. Notably, the commercial adsorbents exhibited suitable properties, aligning with expectations. Furthermore, the synthesized silica aerogels demonstrated properties consistent with existing literature, confirming the successful synthesis of silica aerogels by established previous studies.

3.4 FFA and PV of crude and neutralized sunflower oil

The free fatty acid (FFA) value of crude and neutralized sunflower oil was assessed in the context of adsorption experiments. The FFA value and FFA (%) values of the crude oil utilized in these experiments were 4.72 and 2.37, respectively. In contrast, after neutralization, the FFA value and FFA (%)decreased to 0.56 and 0.28, respectively (Table 2). These values indicate the FFA content within the oil, with a reduction in acid value post-neutralization reflecting a decrease in FFA. The observed decrease in FFA content provides valuable insights into the chemical composition of sunflower oil and the changes it undergoes during the adsorption process.

3.5 Decrease in FFA values in oils after adsorption

Figure 6 illustrates decrease in FFA content following the adsorption of crude sunflower oil using different adsorbent ratios (1–3%) at a temperature of 25 and 90 °C. The adsorption process for all adsorbents except NTSA was performed at 90°C, while the adsorption process with NTSA at various temperatures (25° and 90 °C) was performed. The results showed that FFAs were more effectively adsorbed at higher temperatures compared to lower temperatures for every concentration ($p < 0.05$). This observation confirms consistently with existing literature, highlighting the increased adsorption capability of fatty acids at higher temperatures [110–112]. Consequently, the decision was made to conduct adsorption studies at 90°C for each adsorbent. When employing 1% TSA and NTSA, the FFA value decreased statistically significantly by 20.6% and 23.1%, respectively, compared to crude sunflower oil ($p < 0.05$). Upon increasing the amount of these adsorbents to 3%, the reduction in FFA values rose to 32.2% and

Table 2 FFA and PV value results of crude and neutralized oil

Sunflower oil	FFA value (mg KOH/g)	FFA (%)	PV (mEq/kg)
Crude Oil	4.72 ± 0.02	2.37 ± 0.02	2.10 ± 0.08
Neutralized Oil	0.56 ± 0.01	0.28 ± 0.01	2.64 ± 0.07

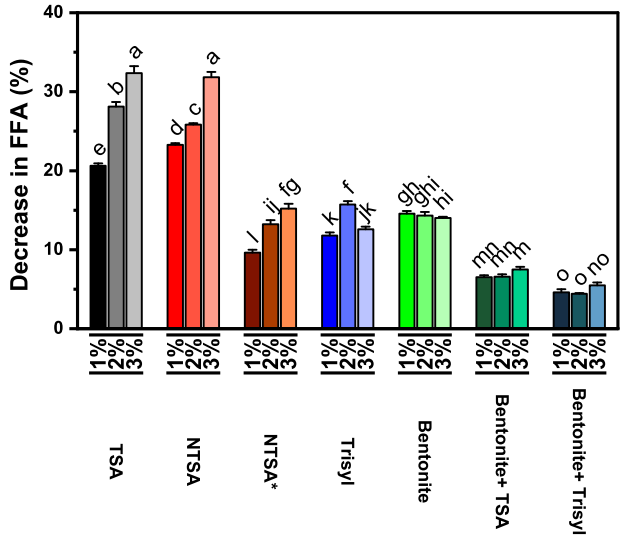

Fig. 6 Decrease in FFA (%) values in crude oil after adsorption for adsorbents (data are given as mean ± SD ($n = 4$)) The different letters on the bar indicate significant differences between values, and the same letters on the bar indicate no difference between values according to Tukey's multiple comparison test ($p < 0.05$). (* shows that adsorption experiments were occurred at 25 °C)

31.8%, respectively. However, there was no statistically significant difference between these two adsorbents at the 3% ratio ($p > 0.05$).

In contrast, 1% and 3% Trisyl exhibited a modest decrease in FFA value with 11.65% and 12.50%, with no statistical significance between ratios ($p > 0.05$), while 1% and 3% Bentonite showed a decrease in FFA value 14.62% and 13.98%, respectively, with no statistical significance between ratios ($p > 0.05$). Furthermore, Bentonite used at the specified ratios exhibited a statistically significant higher adsorption of FFA compared to Trisyl ($p < 0.05$). The observed enhancements could be attributed to the specific adsorption affinity of each adsorbent for acid substances. The different characteristics of each adsorbent could lead to the effective removal of particular molecules, contributing to the overall improvements observed in the process [113–115]. In a study by Boki et al. it was observed that the amount of FFA removal of sepiolite, a clay type, varied between 32% and −4% depending on the type of sepiolite with four wt. % sepiolites in bleaching processes with sunflower oil. This was explained by them as neutral or slightly acidic clays often show a slight reduction in acidity through preferential adsorption of FFAs, as in the literature [116]. It was determined that the FFA adsorption behavior of Bentonite, a type of clay examined in our study, was consistent with the literature. Evaluation of FFA content in crude sunflower oil following adsorption processes revealed statistically significant lower efficacy for both Trisyl and Bentonite compared to the silica aerogel adsorbents at all tested ratios (1–3%) for 90 °C ($p < 0.05$). Trisyl demonstrated the least effectiveness in FFA removal from crude sunflower oil ($p < 0.05$).

Mesoporous silica aerogel adsorbents (NTSA and NSA) exhibit the highest efficacy for removing FFA ($p < 0.05$). Moreover, there is almost no significantly significant correlation between the removal of FFA and the ratio of Trisyl and Bentonite. On the other hand, for mesoporous silica aerogel adsorbents statistically significant correlation with the adsorbent amount is apparent ($p < 0.05$). All these findings indicate that both TSA and NTSA exhibit similarly high efficacy in removing FFAs from crude sunflower oil. Adhikari and his colleagues examined the binding of oleic acid, triacyglycerol and phosphatidycholine on silica at room temperature [117]. They concluded that oleic acid and triacylglycerol bind to the silica surface hydroxyls through hydrogen bond interactions between the carboxylate and ester carbonyls of these molecules, respectively. Similarly, Gil et al. also reported that FFA adsorption on silica-based adsorbents occurs through surface hydrogen bonding between the carboxylic acid groups of FFAs and the silanol (Si-OH) groups present on the silica-based adsorbent surface [118]. Our investigation suggests that similar interactions might be responsible for the adsorption of FFAs onto our silica aerogel adsorbents. In addition, in the study by Schneider et al. stated that RH with low surface area can still be an effective adsorbent for compared to activated carbon with high surface area. This is because the presence of functional groups, active sites, and the overall polarity of the adsorbent also play a crucial role in influencing the adsorbent-adsorbate interaction [68]. Besides, Ahn, and Kwak investigated FFA removal from olive oil using amine-functionalized mesoporous silica with varying pore sizes and specific surface areas. Their study suggests that strong hydrogen bonding and acid-base interactions between on the silica surface and the FFA molecules play a key role in the adsorption process. While surface area plays a part for FFA adsorption, the research indicates that the presence of functional groups on the silica surface has a more significant impact on FFA adsorption [44]. This observation may clarify that Trisyl, despite possessing a higher BET specific surface area, yields lower FFA removal compared to TSA and NTSA. In addition, within the same study, it was noted that among these silica materials, those with higher surface areas (and lower pore diameters) tend to exhibit greater FFA removal. This can be attributed to the fact that TSA and NTSA, which have a similar surface area, provides a similar decrease in FFA.

The presence of ions (Ca or Na in our adsorbents) within the adsorbent structure can potentially contribute to neutralization reactions with FFA. This can establish an acid-base interaction characterized by a rapid equilibrium time. On the other hand, the overall adsorption process might also involve slower chemisorption between the adsorbents and the FFA [67]. Kalapathy and Proctor investigated the use of films obtained from RHA with different silica content for FFA

removal from frying oil [119]. Their findings suggest a positive correlation between Na content in the films and FFA removal efficiency and Na content plays a key role in the FFA removal. According to SEM-EDS (Fig. 4), it was predicted that TSA had more silica content and therefore could adsorb more FFA, while NTSA and TSA were observed to have similar FFA adsorption. While Adhikari et al. stated that the increase in OH groups on silica is expected to be more FFA removal in TSA when it occurs through the mechanism that occurs in silica hydroxyl groups, the reason why it is similar to NTSA may be related to the high Na content of NTSA, as reported by Kalapathy and Proctor [119].

Figure 6 also displays decrease in FFA values following the adsorption of crude sunflower oil, employing combinations adsorbents of Bentonite+TSA and Bentonite+Trisyl. The statically significant lower FFA removing values observed in both combinations compared to the values of the individual adsorbents may be attributed to a negative synergistic effect (an antagonistic effect) arising from the combination of Bentonite with TSA and Trisyl ($p < 0.05$) [9]. Combinations of Bentonite+TSA consistently yielded statistically significant higher FFA removal compared to Bentonite+Trisyl across all studied ratios ($p < 0.05$). However, the increase in FFA removal efficiency between the 1% and 2% ratios for both combinations was relatively small and no statistically significant correlation was observed between the removal of FFAs and the ratio of combinations ($p > 0.05$). All these results suggest that NTSA and TSA can be effectively employed for FFA adsorption when utilized alone.

3.6 Decrease in PV in oils after adsorption

Peroxides represent the initial oxidation products of fatty acids, predominantly generated when partially processed or refined oils interact with air during processing, transportation, and storage [120]. Table 2 provides the PV results for both crude and neutralized sunflower oil, revealing PV values of 2.1 and 2.64, respectively. Additionally, Fig. 7. presents the decrease in PV results of crude sunflower oil after adsorption experiments with TSA, NTSA, Bentonite, Trisyl, and certain combinations at concentrations ranging from 1 to 3%.

Evaluation of individual adsorbent performance for Bentonite, Trisyl, and NTSA adsorbents revealed that a 1% ratio achieved statistically significant higher results for removing PV compared to higher concentrations ($p < 0.05$). Increasing the adsorbent amount from 1% to 3% resulted in a statistically significant decrease in PV removal efficiency for NTSA, Bentonite, and Trisyl ($p < 0.05$). In contrast, TSA exhibited no statistically significant PV removal by increasing the amount of the adsorbent ($p > 0.05$). TSA demonstrated the effective results at for all ratio for removing the PV, with a consistent efficiency level with

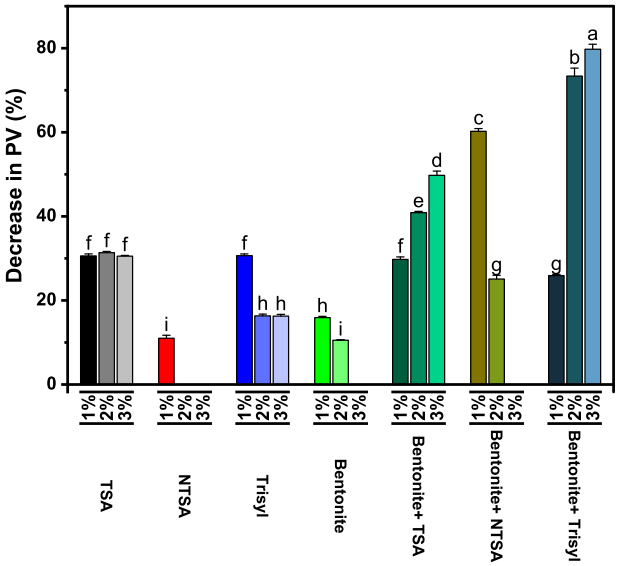

Fig. 7 Decrease in PV (%) value results of crude sunflower oil after adsorption (data are given as mean ± SD ($n = 4$)) The different letters on the bar indicate significant differences between values, and the same letters on the bar indicate no difference between values according to Tukey's multiple comparison test ($p < 0.05$)

increasing ratio. Importantly, both TSA and Trisyl achieved the statistically most significant reductions PV content. Notably, no statistically significant difference was observed between the TSA and Trisyl decrease in PV removal at 1% ratio ($p > 0.05$).

Increase in the surface area of the adsorbent, the amount of peroxide increases up to a certain point, but this does not only sometimes coincide with the highest surface area. The higher peroxide adsorption observed with Trisyl and TSA may be attributed to their relatively higher surface area. Besides, when the removing of PV performances of TSA and NTSA are compared, it is seen that the decrease in the PV value of TSA is statically significance higher ($p < 0.05$). Kalapathy and Proctor investigated the use of silica-based films for reducing PV in frying oil and their findings revealed a decrease in PV for films with high silica content, while films with low silica content exhibited an increase instead of a decrease in PV [119].

As reported in previous studies [121] decomposition products of hydroperoxides, such as aldehydes and ketones, can be adsorbed by the active sites of silica sorbents such as Trisyl. Besides, clays exhibit a dual role in both adsorbing/removing peroxides and catalyzing their conversion into secondary oxidation products. The adsorption capacity of clays for primary and secondary oxidation products is known to have adsorption capacity, which is contingent upon the concentration of the clay [122]. Additionally, Susilowati et al. demonstrated that the removal of peroxides increased up to a certain adsorbent (ampo, a type of clay) concentration. However, beyond this point, the PV removal decreased with a

further increase in the adsorbent amount [123]. The observed decrease in PV% with increasing amounts of Trisyl and Bentonite might be attributed to a common mechanism.

The combined use of adsorbents has yielded favorable results in oil and peroxide adsorption studies. In our study, the impact of Bentonite+TSA, Bentonite+NTSA, and Bentonite+Trisyl combinations decrease in PV was given for crude oil in Table 4. The statistically most significant reduction in PV was achieved using a combination of Bentonite +Trisyl, particularly at the 2% and 3% ratios ($p < 0.05$). This finding suggests a potentially synergistic effect between these two adsorbents in removing peroxide compounds. Interestingly, for the Bentonite+NTSA combination, the best results were obtained at a 1% ratio, surpassing all other 1% adsorbent and adsorbent combinations ($p < 0.05$). Nevertheless, an increase in the amount of the Bentonite+NTSA combination led to a dramatically decrease in the PV of crude oil ($p < 0.05$). In contrast, the removal of PV using the Bentonite+TSA combination exhibited an amount-dependent increase. The most effective result, achieving a statistically significant reduction in PV, was observed with the 3% ratio of Bentonite+TSA ($p < 0.05$). The combined use of Bentonite and Trisyl is commonly preferred in oil refining. Trisyl, a synthetic silica already available in the market and utilized in oil refining, was explicitly designed for peroxide removal [9, 124]. The studies indicated that Trisyl exhibits a high adsorption rate for impurities present in the oil [125]. For this reason, better results were obtained in the Trisyl sample compared to others, except TSA. Farag and Basuny investigated the use of both standard and modified silica adsorbents for PV removal in used sunflower oil and they obtained results removal rates of up to 94%, demonstrating superior performance compared to other cellulose-based adsorbents [126]. The inherent high polarity of TSA likely contributed to its substantial adsorption effect in removing oxidation (like peroxides) products, particularly polar materials, from crude sunflower oil. This characteristic may enhance its effectiveness in adsorbing substances with polar attributes, as defined by IUPAC in 1987. Our findings consistently demonstrate the high efficacy of TSA in removing peroxides from crude sunflower oil. This effectiveness is evident when TSA is used alone, where it achieved statistically significant reductions in PV across all tested ratios, outperforming other adsorbents (except for Trisyl 1% ratio). Notably, TSA also displayed promising results when combined with Bentonite, suggesting its potential for using alone or combined with other adsorbents, such as Bentonite.

3.7 Phosphorus analysis results

Phospholipids constitute essential components of sunflower seeds and can be quantitatively analyzed using chromatographic methods [127, 128]. The phospholipid content in crude sunflower oil typically ranges between 0.5% to 1.2% [129]. Since most phospholipids are hydratable, they can be effectively removed from crude oil through aqueous extraction. Phospholipids are called "gummy substances" due to their sticky nature. This stickiness is a significant concern, especially in edible oils, and the undesirability of phospholipids in these oils is primarily attributed to this characteristic [130, 131]. Phospholipids cause the darkening of oil color by generating dark-colored substances during deodorization. Moreover, their presence in oil composition accelerates oxidative reactions due to the prooxidative nature of the phosphorus within their structure [132]. The phosphorus content in oils is directly proportional to the quantity of phospholipids; therefore, their removal results in a corresponding reduction in phosphorus content. It is crucial for the phosphorus content in edible oils like sunflower oil to be maintained at trace amounts to ensure oil quality and stability [133, 134].

The application of Trisyl in the removal of phospholipids is well-established [50, 135–137]. Our investigation assessed the efficacy of various adsorbents for removing phosphorus from crude sunflower oil. In this study, the efficacy of silica aerogels and Bentonite + silica aerogels in removing phospholipids were studied for the first time. The outcomes of phosphorus analysis after crude sunflower oil adsorption processes were represented in Fig. 8.

Crude sunflower oil had a high phosphorus content, around 1543.4 ppm. In contrast, neutralized oil contains only trace amounts of phosphorus. Minimizing color transformation or fixation caused by phospholipids is crucial during physical oil refining. To achieve this, the phosphorus content of the oil after refining should ideally be below 15 ppm, with even lower levels (less than 5 ppm) being preferable [138]. Both silica aerogels (TSA and NTSA) and Trisyl exhibited remarkable efficacy in phospholipid removal when employed individually compared to Bentonite and their combinations ($p < 0.05$). Notably, these adsorbents achieved near-complete adsorption of phospholipids (under detection point), even at a low adsorbent amount of 1%. When comparing single uses in adsorption experiments in crude oil for phosphorus removal, no statistically significant difference was observed between TSA, NTSA, and Trisyl ($p > 0.05$). Silica-based materials exhibit a high capacity for rapid phosphorus adsorption. This can be attributed to the significant initial concentration difference of phosphorus between the solid adsorbents (silica) and liquid phases (oil), leading to a strong concentration gradient that drives the mass transfer process [139]. However, when their combinations with Bentonite were compared, it was revealed that combination of Bentonite+TSA and Bentonite+NTSA achieved the most significant reduction in phosphorus content, reaching approximately

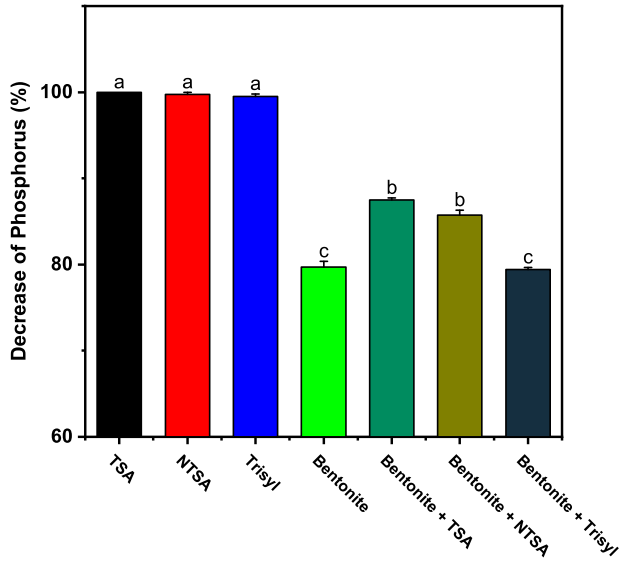

Fig. 8 Decrease of Phosphorus (%) of crude sunflower oil after adsorption (Adsorbent amount was 1 wt. %). (data are given as mean ± SD ($n = 4$)) The different letters on the bar indicate significant differences between values, and the same letters on the bar indicate no difference between values according to ANOVA one way Tukey's comparison test ($p < 0.05$)

87.4% and 85.8% respectively ($p < 0.05$). In this context, TSA and NTSA have demonstrated superior effectiveness compared to Trisyl, which is specifically designed for the removal of phosphorus. In addition, the enhanced adsorption ability of activated bleaching clays was attributed to their acidic properties, where protons and hydrated aluminum ions balance the negative charge of acid-activated montmorillonite [140].

The popular pattern for competitive adsorption of vegetable oil species was consistently ranked as Phospholipid > FFA > PV as shown to be with the relative polarity of the adsorbing functional groups, namely phosphate > carbonyl > peroxide [141]. The reason why TSA, NTSA and Trisyl provide similar phospholipid removal may be due to the competitive order mentioned above. The adsorption of phospholipids to a polar surface predominantly occurs via phosphate group, and this binding is recognized to be more robust than that of FFA or triglycerides to polar OH surface. The enhanced ability of TSA to bind more FFA than other adsorbents, along with its superior peroxide binding compared to NTSA, could potentially be attributed to the availability of excess adsorption sites not realized on other adsorbents after phospholipid and FFA adsorption equilibria were achieved, respectively [142]. Additionally, the silanol groups of silicic acid at the edges of activated montmorillonite were informed to contribute to this more remarkable adsorption ability [140]. SEM-EDS results of the TSA and NTSA indicate that the presence of Na ions in RHA-based silica aerogels might lead to more effective phosphorus adsorption compared to Trisyl (Fig. 4 insets). The comprehensive results indicate that both silica aerogels yield outstanding results in removing phospholipids when used alone. This property is essential in preventing the oil from settling at the bottom during storage, contributing to the stability of the oil.

3.8 Color analysis results of sunflower oil after adsorption

Bleaching is a crucial process aimed at removing color pigments (particularly chlorophyll, gossypol, and carotenoids), along with various impurities such as oxidation products (peroxides) from neutralized oils [143, 144]. This process holds significant importance as it enhances the oxidative stability and sensory qualities of the oil [145]. Activated clays, such as Bentonite, can adsorb color pigments. This capability stems from their adsorption capacity, high surface area, and acidity [146–148]. Activated clays are particularly favored for treating vegetable oils due to their high specificity, enhanced chemical activity, and efficiency [112]. Nevertheless, researchers strive to produce commercial, consumer-standard edible oils utilizing various bleaching agents and processes [149–152]. During the bleaching process in oils, three primary mechanisms govern adsorption during oil bleaching (i) Physical adsorption, involves weak van der Waals forces attracting compounds to the adsorbent surface (ii) Chemisorption, Chemisorption: involves the formation of stronger electrochemical bonding between the compounds and the adsorbent surface (iii) Filtration, involves by molecular sieves which trap contaminants under pressure inside the pores of the clay during filtration [153]. The results of color analysis for oils subjected to adsorption with neutralized sunflower oil, utilizing various adsorbents individually and in combination for the bleaching process, are presented in Table 3. Following the color analysis utilizing the Lovibond tintometer device, it was noted that each of the employed adsorbents demonstrated a varying ratio of efficacy in removing color. The preeminent commercially preferred adsorbent, Bentonite, exhibited a significant reduction for all adsorbent ratios in color units Red (R) and Yellow (Y) components, respectively) from 3.20 ± 0.18 and 30.25 ± 0.83 in neutralized oil to 2.00 ± 0.05 and 19.80 ± 0.54 respectively. The increase in the amount of both Bentonite and TSA did not exhibit statistically significant impact on the levels of R and Y color removal ($p > 0.05$). Traditional bleaching theory suggests a positive correlation between the activity of acid-activated clays, like Ca-Bentonite, and their capacity to remove organic impurities in bleaching process. However, this enhanced activity in highly activated clays can also have negative effects on oil quality and color, ultimately its activity is limited [138]. As commonly known, interlayer

Table 3 Results of color analysis for neutralized oil (data are given as mean ± SD ($n = 4$))

	Adsorbent Amount (wt .%)	Red (R)	Yellow (Y)
Neutralized Oil		3.20 ± 0.18	30.25 ± 0.83
TSA	1	1.98 ± 0.05, a	21.25 ± 0.29, a
TSA	2	1.98 ± 0.05, a	20.05 ± 0.10, a
TSA	3	2.00 ± 0.02, a	20.00 ± 0.21, a
NTSA	1	3.08 ± 0.10, b	30.75 ± 2.25, b
NTSA	2	2.98 ± 0.10, b	29.25 ± 1.50, b
NTSA	3	2.15 ± 0.17, a	21.50 ± 1.29, a
Bentonite	1	2.00 ± 0.05, a	20.13 ± 0.84, a
Bentonite	2	2.00 ± 0.08, a	19.80 ± 0.54, a
Bentonite	3	2.03 ± 0.05, a	20.05 ± 0.22, a
Bentonite + NTSA	1	1.25 ± 0.17, c	10.13 ± 1.03, c
Bentonite + NTSA	2	1.95 ± 0.13, a	20.25 ± 1.26, a
Bentonite + NTSA	3	1.95 ± 0.10, a	19.50 ± 0.58, a
Bentonite + Trisyl	1	1.55 ± 0.06, d	11.25 ± 1.50, c
Bentonite + Trisyl	2	2.03 ± 0.13, a	20.75 ± 0.98, a
Bentonite + Trisyl	3	1.98 ± 0.12, a	21.50 ± 1.00, a

Different letters in the column indicate significant differences between values, and the same letters in the column indicate no difference between values according to Tukey's multiple comparison test ($p < 0.05$)

cations and related acidity values of acid activity clays determine the pigment adsorption capacity [39]. Taylor and Jenkins noted that clays with Al^{3+} and Mg^{2+} exchange ions exhibited superior adsorption of carotene compared to other ions. Besides, clays containing Ca^{2+} and Na^{+} ions showed similar adsorption behavior for carotene [154]. This similarity might explain the closely matched color adsorption observed between Ca Bentonite and TSA, which contains Na^{+} residues in their structure. Moreover, the result of the TSA was also found to be as effective as Bentonite in all ratios for color removal ($p > 0.05$). NTSA demonstrated a statistically significant lower efficacy in R and Y color removal compared to both Bentonite and TSA for 1% and 2% ratios ($p < 0.05$), although it still exhibited effective bleaching. Despite the superior performance of the 1% Bentonite + NTSA combination in neutralized oil, the incremental increase in adsorbent concentration negatively affected color removal while 2% and 3% for Bentonite + NTSA combination result were not statistically significant compared to Bentonite and TSA alone. Similar results and trends emerged in the Bentonite+Trisyl combination regarding color removal efficacy. Our results regarding the enhanced performance of Trisyl in combination with Bentonite at lower ratio are corroborated by the findings of Rincón et al. [50]. Their study also reported similar advantages for this combined adsorbent system in UCO (Used Cooking Oil) refining, highlighting its potential for effectively bleaching slightly dark colored products. The study of Siew et al. [155] researched the removal of color, phosphorus, and iron from palm oil by combining bleaching earth and Trisyl. Similar to our study, the combination of Trisyl and clay was notably reported to enhance refining capabilities, particularly for color removal. Their findings highlighted the capacity of silica to increase the bleaching earth's efficiency in eliminating color bodies and other minor components that influence the color stability of the oil. Nevertheless, it's important to note that this approach may not be economically viable for oil refining, as the cost of Trisyl is three times higher than that of bleaching earths [155]. The study conducted by Yao et al. [156] observed that silicon dioxide reduced the R value of rapeseed oil with an increasing concentration (up to 1.5%). In contrast, no significant effect was observed on the Y value. Another study indicated that the pore size distribution and specific surface area of an adsorbent known as attapulgite are critical parameters influencing the oil bleaching results [157]. The findings revealed that the adsorbents with a pore size suitable for color pigments exhibited the highest color absorption, contrary to samples with the highest surface area or most prominent pores. The efficiency of color removal by adsorbents may be influenced by the size of the color pigment relative to the adsorbent pore diameter. When the pore diameter is significantly larger than the pigment molecules, the pigments can easily pass through the pore interior. Conversely, pores that are too small may restrict color pigment access to the internal adsorption sites. Additionally, larger pores can potentially facilitate desorption of previously adsorbed pigments back into the oil, thus reducing overall color removal [44]. Mesoporous silica with a pore diameter of 6–10 nm exhibited greater efficacy in chlorophyll, which is an effective pigment in color content for oil, removal compared to silica with a pore diameter of 2 nm. Among the TSA and NTSA adsorbents having values between these pore diameter sizes, TSA was highly effective in color removal, whereas NTSA was not as effective as the other adsorbents. Hence, color removal from sunflower oil outcomes may be influenced not solely by the silicon dioxide structures of the silica aerogels but also by the textural properties of the adsorbents. In summary, TSA is effective adsorbents in sunflower oil bleaching, like Bentonite. A noticeable decrease in color values was observed using 1–3% of TSA, while NTSA showed the same performance as TSA for removing color pigments with just a 3% amount.

Table 4 Comparison of FFA, PV, phosphorus, and color adsorption efficiency of different adsorbents[a]

Adsorbent	FFA*	PV*	Phosphorus*	color*
TSA	++	++	++	++
NTSA	++	+	++	+
Trisyl (synthetic silica)[b]	+ [161]	+ [162], [163]	++ [155] [163]	+ [135]
Natural Bentonite[b]	+ [135]	+ [135]	+	++ [164]
Magnesol (Synthetic magnesium silica)	++ [117], [161], [164], [165],	++ [117], [166]	++ [167]	+ [135]
Rice Hull Silica	+ [163], [118]	+ [163]	+ [163]	+ [118], [168]
Silica gel	+ [118], [169]	+ [117], [170]	n.s.	++ [126], [170]
Natural Zeolite	+ [118], [171], [172]	+ [172]	+ [139]	+ [172]
Natural Sepiolite	+ [149]	+ [149]	++ [149]	++ [149]
Mesoporous Silica Nanoparticle	++ [44]	− [44]	n.s.	++ [44]

*(−) ineffective, (+) limited effect, (++) effective, (n.s.) non studied

[a]An evaluation of the effect was conducted utilizing the findings of the present study

[b]The adsorption efficacy of Trisyl and Bentonite was assessed by integrating the outcomes of the present study and information derived from relevant literature sources

The adsorption performances of silica aerogels produced within the scope of the study were compared with those of some adsorbents commercially used (Bentonite, Trisyl) or literature sources in edible oil refining (see Table 4). Upon comprehensive evaluation of the present study findings and the efficacy of adsorbents reported in the literature, silica aerogel demonstrates notable efficiency in removing FFA, peroxides, phosphorus, and color pigments from oils. Moreover, compared with other adsorbents, silica aerogel exhibits high efficacy when used alone, obviating the need for combination with alternative adsorbents. This characteristic can offer commercial convenience due to its ease of application. Our findings indicate that the TSA adsorbents demonstrates most effective performance across all investigated edible oil refining steps compared to NTSA and other adsorbents. This efficacy suggests its potential for oil refining processes by potentially consolidating multiple adsorption steps into a single, unified edible oil refining process using TSA.

3.9 Oil Loss during adsorption

While attempting to remove certain impurities from the oil through adsorption studies, it is known that adsorbent used results in some loss of oils. Minimizing this loss is crucial regarding the overall cost considerations of obtaining edible oil production [37, 158]. As seen in Table 5, as predicted in the oil adsorption process, it was found that the amount of oil lost increased as more adsorbent was used in both crude and neutralized oil studies ($p < 0.05$). This increase was ascribed to the entrapment of oils within the solid adsorbents, aligning with findings reported in existing literature [50]. The data indicates that Trisyl exhibit statistically lowest levels crude oil loss compared to the other samples investigated, whereas the TSA and NTSA samples demonstrate the highest loss of crude oil. Although innovative refining processes reduce oil loss to as low as 0.37 wt.%, traditional methodologies employed in the refining of vegetable oils customarily result in discernible oil losses, typically ranging between 2 and 5 wt.% [159]. Our observations revealed that the RHA-based silica aerogels synthesized in our study exhibited a similar value to those encountered in conventional refining processes, particularly within the 2 wt.% threshold. However, it should be noted that refining losses may be higher if the FFA content in vegetable oils is high [160]. As anticipated, both Trisyl and Bentonite demonstrated values below these values. NTSA is chemically similar to TSA, and TSA shows similar results to NTSA in oil loss. Besides, the adsorption studies conducted on crude oil at both 90 °C and 25 °C, as illustrated in Fig. 6., revealed that when comparing the results of NTSA used at the same rate, it was evident that a slightly more significant amount of oil was adsorbed in the process conducted at 90 °C while our data revealed no statistically significant difference in oil loss between the adsorption processes conducted at 90 °C and 25 °C ($p > 0.05$). This outcome indicates that the optimal conditions for edible oil processes, ensuring high FFA removal and low oil loss, involve performing the process at high temperatures. When the combinations are examined, the lowest oil loss is observed in Bentonite+Trisyl because Trisyl causes lower oil loss when used alone ($p < 0.05$). The combination of Bentonite with either TSA or NTSA resulted in similar oil loss levels. Notably, these combined adsorbents exhibited significantly lower oil loss compared to using TSA or NTSA alone. The inherent low-oil loss characteristic of

Table 5 Oil losses in crude and neutralized sunflower oil during adsorption process (data are given as mean ± SD ($n = 4$))

Adsorbents	Adsorbent Amount (wt .%)	Losses in crude oil (%)	Losses in neutralized oil (%)
TSA	1	2.49 ± 0.14, g	3.31 ± 0.08, hi
TSA	2	3.98 ± 0.21, d	4.63 ± 0.07, de
TSA	3	5.57 ± 0.49, b	6.99 ± 0.34, a
NTSA	1	2.70 ± 0.58, g	3.90 ± 0.07, g
NTSA	2	4.13 ± 0.25, cd	4.96 ± 0.12, d
NTSA	3	6.28 ± 0.48, a	6.01 ± 0.16, b
NTSA*	1	2.37 ± 0.13, g	3.54 ± 0.07, h
NTSA*	2	3.87 ± 0.06, d	4.27 ± 0.06, f
NTSA*	3	5.79 ± 0.15, ab	5.45 ± 0.16, c
Bentonite	1	1.40 ± 0.11, kl	1.96 ± 0.05, mn
Bentonite	2	2.33 ± 0.12, gh	2.23 ± 0.10, lm
Bentonite	3	3.02 ± 0.10, ef	2.82 ± 0.17, jk
Trisyl	1	1.06 ± 0.11, l	0.69 ± 0.04, q
Trisyl	2	1.56 ± 0.51, jk	1.41 ± 0.03, p
Trisyl	3	2.15 ± 0.05, gh	2.24 ± 0.10, lm
Bentonite + TSA	1	1.74 ± 0.13, jk	2.34 ± 0.03, l
Bentonite + TSA	2	3.08 ± 0.22, ef	3.17 ± 0.14, I
Bentonite + TSA	3	4.37 ± 0.11, cd	4.51 ± 0.14, ef
Bentonite + NTSA	1	1.93 ± 0.10, ij	2.45 ± 0.10, l
Bentonite + NTSA	2	3.26 ± 0.17, e	3.05 ± 0.11, ij
Bentonite + NTSA	3	4.64 ± 0.10, c	4.74 ± 0.16, de
Bentonite + Trisyl	1	1.23 ± 0.06, kl	1.53 ± 0.11, op
Bentonite + Trisyl	2	2.18 ± 0.17, gh	1.80 ± 0.05, no
Bentonite + Trisyl	3	3.09 ± 0.08, ef	2.50 ± 0.10, kl

Different letters in the column indicate significant differences between values, and the same letters in the column indicate no difference between values according to Tukey's multiple comparison test ($p < 0.05$). (* shows that adsorption experiments were occurred at 25 °C)

Bentonite, observed when used independently, appears to be reduced when combined with other substances.

Adsorption studies conducted with neutralized oil represented the lowest oil loss at a 1% Trisyl ratio, similar the results observed with crude oil. This suggests that the presence of different compounds in crude oil may not significantly influence oil loss of Trisyl (Table 5). In a manner similar to the outcomes observed with crude oil, TSA exhibited the highest oil loss during refining process. Notably, the combination of Bentonite with silica aerogel adsorbents resulted in a decrease in oil loss compared to using Bentonite alone. However, this trend was not observed for the Bentonite-Trisyl combination. Bentonite combinations with other adsorbents exhibited results closely mirroring those of the individual adsorbents themselves, indicating a significant similarity in their oil adsorption capabilities, particularly in a combination. The findings suggest that the TSA can be said to display a moderate oil loss in applications involving oil adsorption, albeit higher when compared to other adsorbents. This could be attributed to its strong oil refining capacity, particularly in the removal of FFA, PV, and phosphorus. Consequently, this highlights the suitability of TSA for either itself use or in combination with Bentonite for oil adsorption applications. The potential of TSA, whether employed itself use or in combination with Bentonite, underscores its high efficacy in addressing diverse challenges associated with oil adsorption under various conditions.

4 Conclusion

In conclusion, our comprehensive adsorption experiments including removing of FFA, peroxides, phosphorous and color on sunflower oil, employing various weight ratios of non-TEOS-doped silica aerogel, TEOS-doped silica aerogel, Trisyl, and Bentonite, revealed important insights into the efficacy of these adsorbents. In the present study, the influence of TEOS doping during the aging phase was examined. Furthermore, a series of adsorption experiments involving both crude and neutralized sunflower oil, different adsorption temperatures, and using various weight ratios of adsorbents such as silica aerogels (TEOS-doped and non-TEOS-doped), Trisyl, and Bentonite, were successfully conducted. The results of BET analysis revealed that the doping of TEOS during the aging phase increased the surface area of silica aerogels. TEOS-doped silica aerogel used alone has proven to be more effective in FFA removal than Trisyl and Bentonite under the same conditions. In terms of PV, TEOS-doped silica aerogel was observed very efficient compared to other adsorbents and the combination of Bentonite+Trisyl demonstrated optimal results. Both silica aerogel as well as Trisyl significantly reduced the phosphorus content of crude oil. In the bleaching step, TEOS-doped mesoporous silica aerogel exhibited similar efficacy to Bentonite. Overall, TEOS-doped silica aerogel had the potential to serve as efficacious adsorbents in the physical refining of sunflower oil for the removal of undesirable compounds. Furthermore, the incorporation of additional ions into silica aerogels or modifying silica aerogels can provide for enhancing their efficacy. This might open up possibilities for the development of

adsorbents capable of executing numerous oil refining processes concurrently in a singular step.

Data availability

The authors confirm that the data supporting the findings of this study are available within the article. Raw data that support the findings of this study are available from the corresponding author, upon reasonable request.

Code availability

The authors confirm that the data supporting the findings of this study are available within the article. Raw data that support the findings of this study are available from the corresponding author, upon reasonable request.

Acknowledgements This work has been supported by Yildiz Technical University Scientific Research Projects Coordination Unit under project number 2015-07-04-KAP05. Tülay Merve TEMEL-SOYLU would like to thank the financial support by the Council of Higher Education (YÖK) under the YÖK 100/2000 National PhD Scholarship Program. Cem ÖZEL also thanks the financial support from the Scientific and Technological Research Council of Turkey (TÜBİTAK) under the BIDEB/2211-A National PhD Scholarship Program and Ali Can Özarslan and Cem ÖZEL BIDEB/2250 - Performance-Based Scholarships Program for PhD.

Author contributions SY conceived the idea and supervised the project. TMTS, BK, and YE synthesized silica aerogels. TMTS, BK, PT and YE studied adsorption experiments. CÖ and ACÖ studied the characteristics of the adsorbents by different techniques. TMTS, BK and PT writing original draft.YE and SY supervised the findings of this work and discussed the results. TMTS, CÖ, ACÖ and SY contributed to the final paper for reviewing and editing.

Funding Open access funding provided by the Scientific and Technological Research Council of Türkiye (TÜBİTAK).

Compliance with ethical standards

Conflict of interest The authors declare no competing interests.

Publisher's note Springer Nature remains neutral with regard to jurisdictional claims in published maps and institutional affiliations.

References

1. Noman MT, Amor N, Ali A et al.(2021) Aerogels for Biomedical, Energy and Sensing Applications. Gels 7:264. https://doi.org/10.3390/GELS7040264
2. Twumasi Afriyie E (2013) Preparation and Evaluation of New Nanoporous Silica Materials for Molecular Filtration and for Core Materials in Vacuum Insulation Panels. KTH Royal Institute of Technology, Sweden
3. Lee KH, Arshad Z, Dahshan A et al.(2023) Porous Aerogel Structures as Promising Materials for Photocatalysis, Thermal Insulation Textiles, and Technical Applications: A Review Catalyst 13:1286. https://doi.org/10.3390/CATAL13091286
4. Tiryaki E, Özarslan AC, Yücel S, Correa-Duarte MA (2023) Plasmon-Sensitized Silica-Titanium Aerogels as Potential Photocatalysts for Organic Pollutants and Bacterial Strains. ACS Omega 8:33857–33869. https://doi.org/10.1021/ACSOMEGA.3C04556/ASSET/IMAGES/LARGE/AO3C04556_0007.JPEG
5. Tiryaki E, Başaran Elalmış Y, Karakuzu İkizler B, Yücel S (2020) Novel organic/inorganic hybrid nanoparticles as enzyme-triggered drug delivery systems: Dextran and Dextran aldehyde coated silica aerogels. J Drug Deliv Sci Technol 56:101517. https://doi.org/10.1016/J.JDDST.2020.101517
6. Michaloudis I, Skouloudi M, Bok C, Jingyan Q (2017) Spirited Skies Project: Silica Aerogel Domes for the Habitat of the Future. Adv Automob Eng 6:1–7. https://doi.org/10.4172/2167-7670.1000166
7. Karimi M, Shirzad M, Silva JAC, Rodrigues AE (2022) Biomass/Biochar carbon materials for CO2 capture and sequestration by cyclic adsorption processes: A review and prospects for future directions. J CO2 Util 57:101890. https://doi.org/10.1016/J.JCOU.2022.101890
8. Karimi M, Shirzad M, Silva JAC, Rodrigues AE(2023) Carbon dioxide separation and capture by adsorption: a review Environ Chem Lett 21:2041–2084. https://doi.org/10.1007/S10311-023-01589-Z
9. Rossi M, Gianazza M, Alamprese C, Stanga F (2003) The role of bleaching clays and synthetic silica in palm oil physical refining. Food Chem 82:291–296. https://doi.org/10.1016/S0308-8146(02)00551-4
10. Hebalkar N, Kollipara KS, Ananthan Y, Krishna Sudha M (2020) Nanoporous Aerogels for Defense and Aerospace Applications. Handb Adv Ceram Compos Defense, Secur Aerosp Energy Appl 121–163. https://doi.org/10.1007/978-3-030-16347-1_5/FIGURES/13
11. Franco P, Cardea S, Tabernero A et al.(2021) Porous Aerogels and Adsorption of Pollutants from Water and Air: A Review. Molecules 26:4440. https://doi.org/10.3390/MOLECULES26154440
12. Çok SS, Koç F, Len A, et al (2023) The role of surface and structural properties on the adsorptive behavior of vinyl-methyl decorated silica aerogel-like hybrids for oil/organic solvent clean-up practices. Sep Purif Technol 125958. https://doi.org/10.1016/J.SEPPUR.2023.125958
13. Faghihian H, Nourmoradi H, Shokouhi M (2014) Removal of copper (II) and nickel (II) from aqueous media using silica aerogel modified with amino propyl triethoxysilane as an adsorbent: equilibrium, kinetic, and isotherms study. Desalin Water Treat 52:305–313. https://doi.org/10.1080/19443994.2013.785367
14. Pouretedal HR, Kazemi M (2012) Characterization of modified silica aerogel using sodium silicate precursor and its application as adsorbent of Cu2+, Cd2+, and Pb2+ ions. Int J Ind Chem 3:1–8. https://doi.org/10.1186/2228-5547-3-20/TABLES/4

15. Gurav JL, Jung IK, Park HH, et al. (2010) Silica aerogel: Synthesis and applications. J Nanomater 2010: https://doi.org/10.1155/2010/409310
16. Soleimani Dorcheh A, Abbasi MH (2008) Silica aerogel; synthesis, properties and characterization. J Mater Process Technol 199:10–26. https://doi.org/10.1016/J.JMATPROTEC.2007.10.060
17. Rao AV, Pajonk GM, Bangi UKH, et al (2011) Sodium Silicate Based Aerogels via Ambient Pressure Drying. In: Aegerter MA, Leventis N, Koebel MM (eds) Aerogels Handbook. Springer, New York, NY, pp 103–124
18. Sethy NK, Arif Z, Mishra PK, Kumar P (2019) Synthesis of SiO2 nanoparticle from bamboo leaf and its incorporation in PDMS membrane to enhance its separation properties. J Polym Eng 39:679–687. https://doi.org/10.1515/POLYENG-2019-0120/MACHINEREADABLECITATION/RIS
19. Lu Y, Liu Z, Li X et al. (2022) Development of water-based thermal insulation paints using silica aerogel made from incineration bottom ash. Energy Build 259:111866. https://doi.org/10.1016/J.ENBUILD.2022.111866
20. Yadav VK, Fulekar MH (2019) Green synthesis and characterization of amorphous silica nanoparticles from fly ash. Mater Today Proc 18:4351–4359. https://doi.org/10.1016/J.MATPR.2019.07.395
21. Farirai F, Mupa M, Daramola MO (2021) An improved method for the production of high purity silica from sugarcane bagasse ash obtained from a bioethanol plant boiler. Part Sci Technol 39:252–259. https://doi.org/10.1080/02726351.2020.1734700
22. He P, Gao XD, Li XM et al. (2014) Highly transparent silica aerogel thick films with hierarchical porosity from water glass via ambient pressure drying. Mater Chem Phys 147:65–74. https://doi.org/10.1016/J.MATCHEMPHYS.2014.04.007
23. Karakuzu Ikizler B, Yapıcı E, Yücel S, Ermiş E (2023) Production and Characterization of Calcium Silica Aerogel Powder as a Food Additive. ACS Omega 8:11479–11491. https://doi.org/10.1021/ACSOMEGA.3C00358/ASSET/IMAGES/LARGE/AO3C00358_0014.JPEG
24. Kılıç E, Akyol E, Karakuzu-İkizler B et al. (2020) Production of Novel Composite Films Based on PVA-Biosilica. J Indian Chem Soc 97:2092–2096
25. Abbas N, Khalid HR, Ban G et al. (2019) Silica aerogel derived from rice husk: an aggregate replacer for lightweight and thermally insulating cement-based composites. Constr Build Mater 195:312–322. https://doi.org/10.1016/J.CONBUILDMAT.2018.10.227
26. Muhammad S, Yahya EB, Abdul Khalil HPS et al.(2023) Recent Advances in Carbon and Activated Carbon Nanostructured Aerogels Prepared from Agricultural Wastes for Wastewater Treatment Applications Agriculture 13:208. https://doi.org/10.3390/AGRICULTURE13010208
27. Nassar MY, Ahmed IS, Raya MA (2019) A facile and tunable approach for synthesis of pure silica nanostructures from rice husk for the removal of ciprofloxacin drug from polluted aqueous solutions. J Mol Liq 282:251–263. https://doi.org/10.1016/J.MOLLIQ.2019.03.017
28. Abdul Razak NA, Othman NH, Mat Shayuti MS et al. (2022) Agricultural and industrial waste-derived mesoporous silica nanoparticles: A review on chemical synthesis route. J Environ Chem Eng 10:107322. https://doi.org/10.1016/J.JECE.2022.107322
29. USDA (United State of Department of Agriculture) (2023) Rice Production by Country | World Agricultural Production 2023/2024. http://www.worldagriculturalproduction.com/crops/rice.aspx. Accessed 19 Dec 2023
30. Halim ZAA, Awang N, Ahmad N, Yajid MAM (2022) Effects of silane concentration on hydrophobic conversion of rice husk-derived silica aerogels prepared by supercritical drying. Biomass Convers Biorefinery 1:1–11. https://doi.org/10.1007/S13399-022-03710-8/FIGURES/11
31. Romasanta RR, Sander BO, Gaihre YK et al. (2017) How does burning of rice straw affect CH4 and N2O emissions? A comparative experiment of different on-field straw management practices. Agric Ecosyst Env 239:143–153. https://doi.org/10.1016/j.agee.2016.12.042
32. Karaca AE, Özel C, Özarslan AC, Yücel S (2022) The simultaneous extraction of cellulose fiber and crystal biogenic silica from the same rice husk and evaluation in cellulose-based composite bioplastic films. Polym Compos 43:6838–6853. https://doi.org/10.1002/PC.26729
33. Karakuzu B, Temel TM, Yucel S et al. (2016) Effect of acid type and gelation pH on the structural properties of silica aerogels prepared by use of rice hull biosilica. Sigma J Eng Nat Sci Mühendislik ve Fen Bilim Derg 34:175–182
34. Chen K, Feng Q, Feng Y et al. (2022) Ultrafast removal of humic acid by amine-modified silica aerogel: Insights from experiments and density functional theory calculation. Chem Eng J 435:135171. https://doi.org/10.1016/J.CEJ.2022.135171
35. Zulfiqar U, Subhani T, Wilayat Husain S (2015) Towards tunable size of silica particles from rice husk. J Non Cryst Solids 429:61–69. https://doi.org/10.1016/J.JNONCRYSOL.2015.08.037
36. Nzereogu PU, Omah AD, Ezema FI et al. (2023) Silica extraction from rice husk: Comprehensive review and applications. Hybrid Adv 4:100111. https://doi.org/10.1016/J.HYBADV.2023.100111
37. Gharby S (2022) Refining Vegetable Oils: Chemical and Physical Refining. Sci World J 2022: https://doi.org/10.1155/2022/6627013
38. Pan F, Li Y, Luo X et al. (2020) Effect of the chemical refining process on composition and oxidative stability of evening primrose oil. J Food Process Preserv 44:e14800. https://doi.org/10.1111/JFPP.14800
39. Swern D (1982) Bailey's industrial oil and fat products. John Wiley and Sons, Inc, New York, NY
40. O'Brien RD (2008) Soybean Oil Purification. Soybeans Chem Prod Process Util 377–408. https://doi.org/10.1016/B978-1-893997-64-6.50015-9
41. Wongsurakul P, Termtanun M, Kiatkittipong W et al.(2022) Comprehensive Review on Potential Contamination in Fuel Ethanol Production with Proposed Specific Guideline Criteria. Energies 15:2986. https://doi.org/10.3390/EN15092986
42. Marone PA, Birkenbach VL, Hayes AW (2016) Newer Approaches to Identify Potential Untoward Effects in Functional Foods. Int J Toxicol 35:186–207. https://doi.org/10.1177/1091581815616781/ASSET/IMAGES/LARGE/10.1177_1091581815616781-FIG1.JPEG
43. Vera C, Busto M, Yori J, et al. (2011) Adsorption in Biodiesel Refining - A Review. Biodiesel - Feed Process Technol. https://doi.org/10.5772/26587
44. Ahn Y, Kwak SY (2020) Functional mesoporous silica with controlled pore size for selective adsorption of free fatty acid and chlorophyll. Microporous Mesoporous Mater 306:110410. https://doi.org/10.1016/J.MICROMESO.2020.110410
45. Dülger A, Yilmaz E (2013) Effectiveness of modified zeolites as adsorbent materials for frying oils. Eur J Lipid Sci Technol 115:668–675. https://doi.org/10.1002/ejlt.201200312
46. Khok YT, Ooi CH, Matsumoto A, Yeoh FY (2020) Reactivation of spent activated carbon for glycerine purification. Adsorption 26:1015–1025. https://doi.org/10.1007/S10450-020-00210-X/FIGURES/15
47. Deng M, Zhou A, Cheng C et al. (2020) Role of polyurethane-modified layered double hydroxides on SCFAs extraction from

waste activated sludge fermentation liquid for elevating denitrification: Kinetics and mechanism. Environ Res 187:109696. https://doi.org/10.1016/J.ENVRES.2020.109696
48. Wu Z, Li C, Sun X et al. (2006) Characterization, Acid Activation and Bleaching Performance of Bentonite from Xinjiang. Chinese J Chem Eng 14:253–258. https://doi.org/10.1016/S1004-9541(06)60067-0
49. Usman MA, Oribayo O, Adebayo AA (2013) Bleaching of palm oil by activated local bentonite and kaolin clay from Afashio, Edo-Nigeria. Chem Process Eng Res 10:1–12
50. Rincón LA, Ramírez JC, Orjuela A (2021) Assessment of degumming and bleaching processes for used cooking oils upgrading into oleochemical feedstocks. J Environ Chem Eng 9:104610. https://doi.org/10.1016/J.JECE.2020.104610
51. Čmolík J, Pokorný J (2000) Physical refining of edible oils. Eur J Lipid Sci Technol 102:472–486
52. Tse TJ, Zhou L, Chicilo F, et al. (2023) Biodiesel Refining and Processing Strategies. In: Fattah IMR (ed) Advanced Biodiesel - Technological Advances, Challenges, and Sustainability Considerations. IntechOpen
53. W. R. Grace & Co.-Conn (2023) TRISYL® Silica for Edible Oil Refining. https://grace.com/industries/food-beverage/edible-oil-refining/. Accessed 19 Dec 2023
54. Al-Dabbas MM, Al-Jaloudi R, Abdullah MA, Abughoush M(2023) Characterization of Olive Oil Volatile Compounds after Elution through Selected Bleaching Materials—Gas Chromatography–Mass Spectrometry Analysis Molecules 28:6444. https://doi.org/10.3390/MOLECULES28186444
55. Shi L, Cui Z, Liu W(2023) (2023) Effect of Chemical Refining on the Reduction of β-Carboline Content in Sesame Seed Oil Molecules 28:4503. https://doi.org/10.3390/MOLECULES28114503
56. Igansi AV, Engelmann J, Lütke SF et al. (2019) Isotherms, kinetics, and thermodynamic studies for adsorption of pigments and oxidation products in oil bleaching from catfish waste. Chem Eng Commun 206:1410–1424. https://doi.org/10.1080/00986445.2018.1539965
57. Özgül-Yücel S, Türkay S (2003) Purification of FAME by rice hull ash adsorption. J Am Oil Chem Soc 80:373–376. https://doi.org/10.1007/S11746-003-0706-0
58. Taspinar OO, Ozgul-Yucel S (2008) Lipid adsorption capacities of magnesium silicate and activated carbon prepared from the same rice hull. Eur J Lipid Sci Technol 110:742–746. https://doi.org/10.1002/EJLT.200700313
59. Narenji-Sani F, Tayebee R, Chahkandi M (2020) New Task-Specific and Reusable ZIF-like Grafted H6P2W18O62 Catalyst for the Effective Esterification of Free Fatty Acids. ACS Omega 5:9999–10010. https://doi.org/10.1021/ACSOMEGA.0C00358/ASSET/IMAGES/MEDIUM/AO0C00358_M004.GIF
60. Park JY, Kim DK, Lee JS (2010) Esterification of free fatty acids using water-tolerable Amberlyst as a heterogeneous catalyst. Bioresour Technol 101:S62–S65. https://doi.org/10.1016/J.BIORTECH.2009.03.035
61. Rosales-Solano H, Galievsky V, Murtada K et al. (2022) Profiling of Unsaturated Lipids by Raman Spectroscopy Directly on Solid-Phase Microextraction Probes. Anal Chem 94:606–611. https://doi.org/10.1021/ACS.ANALCHEM.1C04054/ASSET/IMAGES/LARGE/AC1C04054_0004.JPEG
62. Marjani A, Soltani R, Pishnamazi M et al. (2021) Functionalized pollen-like mesoporous silica. Microporous Mesoporous Mater 310:110531. https://doi.org/10.1016/J.MICROMESO.2020.110531
63. Chen J, Lyu Q, Yang M et al. (2016) Selective elimination of the free fatty acid fraction from esterified fatty acids in rat plasma through chemical derivatization and immobilization on amino functionalized silica nano-particles. J Chromatogr A 1431:197–204. https://doi.org/10.1016/J.CHROMA.2015.12.078
64. Cha D, Liu M, Zeng Z et al. (2006) Analysis of fatty acids in lung tissues using gas chromatography–mass spectrometry preceded by derivatization-solid-phase microextraction with a novel fiber. Anal Chim Acta 572:47–54. https://doi.org/10.1016/J.ACA.2006.05.014
65. Zhao Q, Li J, Xu Y et al. (2019) Rapid extraction of free fatty acids from edible oil after accelerated storage based on amino-modified magnetic silica nanospheres. Anal Methods 11:4520–4527. https://doi.org/10.1039/C9AY01082C
66. Wang Y, Yang C, Wang X et al. (2024) Determination of free fatty acids in edible oil based on hollow mesoporous silica nanoparticles. Food Chem 443:138561. https://doi.org/10.1016/J.FOODCHEM.2024.138561
67. Zainal ZS, Hoo P, Ahmad AL et al. (2024) Plant-based calcium silicate from rice husk ash: A green adsorbent for free fatty acid recovery from waste frying oil. Heliyon 10:e26591. https://doi.org/10.1016/J.HELIYON.2024.E26591
68. Schneider LT, Bonassa G, Alves HJ et al. (2019) Use of rice husk in waste cooking oil pretreatment. Environ Technol 40:594–604. https://doi.org/10.1080/09593330.2017.1397772
69. Kalapathy U, Proctor A, Shultz J (2000) A simple method for production of pure silica from rice hull ash. Bioresour Technol 73:257–262. https://doi.org/10.1016/S0960-8524(99)00127-3
70. Temel TM, İkizler BK, Terzioğlu P et al. (2017) The effect of process variables on the properties of nanoporous silica aerogels: an approach to prepare silica aerogels from biosilica. J Sol-Gel Sci Technol 84:51–59. https://doi.org/10.1007/S10971-017-4469-X/FIGURES/6
71. AOCS (1998) Method Ca 5a-40, Official Methods and Recommended Practices of the AOCS
72. Özyurt G, Sakarya Y, Durmuş M (2022) Chemical and physical characterization of spray dried fish oil with different combination ratios of wall component. J Food Process Preserv 46:e17223. https://doi.org/10.1111/JFPP.17223
73. Medeiros Vicentini-Polette C, Rodolfo Ramos P, Bernardo Gonçalves C, Lopes De Oliveira A (2021) Determination of free fatty acids in crude vegetable oil samples obtained by high-pressure processes. Food Chem X 12:100166. https://doi.org/10.1016/J.FOCHX.2021.100166
74. AOCS (1998) Method Cd 8-53, Official methods and recommended practices of the AOCS. American Oil Chemists'. Society, Champaign, IL
75. AOCS (2017) Method Cc 13e-92, Official Methods and Recommended Practices of the AOCS. Am. Oil Chem. Soc
76. AOCS (2021) Method Cc 13j-97, Official Methods and Recommended Practices of the AOCS. Am. Oil Chem. Soc
77. AOCS (2017) Method Cc 13b-45, Offical methods and recommended practices of the AOCS. Am. Oil Chem. Soc
78. Shariff R, Aachary AA, Pacquette LH et al. (2018) Analytical Method Validation and Determination of Iron and Phosphorus in Vegetable Oil by Inductively Coupled Plasma–Mass Spectrometry with Microwave Assisted Digestion. Anal Lett 51:1774–1788. https://doi.org/10.1080/00032719.2017.1387554
79. Matias T, Marques J, Quina MJ et al. (2015) Silica-based aerogels as adsorbents for phenol-derivative compounds. Colloids Surfaces A Physicochem Eng Asp 480:260–269. https://doi.org/10.1016/J.COLSURFA.2015.01.074
80. Yi Z, Tang Q, Jiang T, Cheng Y (2019) Adsorption performance of hydrophobic/hydrophilic silica aerogel for low concentration organic pollutant in aqueous solution. Nanotechnol Rev 8:266–274. https://doi.org/10.1515/NTREV-2019-0025/MACHINEREADABLECITATION/RIS
81. Liao J, Gao P, Xu L, Feng J (2018) A study of morphological properties of SiO2 aerogels obtained at different temperatures. J

Adv Ceram 7:307–316. https://doi.org/10.1007/s40145-018-0280-6
82. Al-Oweini R, El-Rassy H (2009) Synthesis and characterization by FTIR spectroscopy of silica aerogels prepared using several Si(OR)4 and R″Si(OR′)3 precursors. J Mol Struct 919:140–145. https://doi.org/10.1016/j.molstruc.2008.08.025
83. Dziadek M, Zagrajczuk B, Jelen P et al. (2016) Structural variations of bioactive glasses obtained by different synthesis routes. Ceram Int 42:14700–14709. https://doi.org/10.1016/J.CERAMINT.2016.06.095
84. Chungong LF, Isaacs MA, Morrell AP et al. (2019) Insight into the atomic scale structure of CaF2-CaO-SiO2 glasses using a combination of neutron diffraction, 29Si solid state NMR, high energy X-ray diffraction, FTIR, and XPS. Biomed Glas 5:112–123. https://doi.org/10.1515/BGLASS-2019-0010/MACHINEREADABLECITATION/RIS
85. Almeida RM, Marques AC (2018) Characterization of Sol-Gel Materials by Infrared Spectroscopy. In: Klein L, Aparicio M, Jitianu A (eds) Handbook of Sol-Gel Science and Technology: Processing, Characterization and Applications. Springer International Publishing, Cham, pp 1121–1151
86. Özel C, Akat C, Alosmanov R et al. (2021) Surface modification of zeolite and kaolin with 3-(aminopropyl) triethoxysilane and 3-(trimethoxysilyl) propyl methacrylate. Bulg Chem Commun 53:464–470. https://doi.org/10.34049/bcc.53.4.T003
87. Bhatia L, Sahu DK (2023) SEM & FTIR Analysis of Rice Husk to Assess the Impact of Physiochemical Pretreatment. J Agric Ecol Res Int 24:1–13. https://doi.org/10.9734/JAERI/2023/V24I6556
88. Derfus AM, Chan WCW, Bhatia SN (2003) Probing the Cytotoxicity of Semiconductor Quantum Dots. Nano Lett 4:11–18. https://doi.org/10.1021/NL0347334
89. Ciftci F, Özarslan AC (2023) Preparation of PLGA-PEG/Hydroxyapatite Composites via Simple Methodology of Film Formation and Assessment of Their Structural, Thermal, and Biological Features. J Turkish Chem Soc Sect A Chem 10:1123–1132. https://doi.org/10.18596/JOTCSA.1313562
90. Ozder MN, Ciftci F, Rencuzogullari O et al. (2023) In situ synthesis and cell line studies of nano-hydroxyapatite/graphene oxide composite materials for bone support applications. Ceram Int 49:14791–14803. https://doi.org/10.1016/J.CERAMINT.2023.01.075
91. Mannu A, Vlahopoulou G, Sireus V et al. (2018) Bentonite as a Refining Agent in Waste Cooking Oils Recycling: Flash Point, Density and Color Evaluation. Nat Prod Commun 13:613–616. https://doi.org/10.1177/1934578X1801300523
92. Alemdar A, Güngör N, Ece OI, Atici O (2005) The rheological properties and characterization of bentonite dispersions in the presence of non-ionic polymer PEG. J Mater Sci 40:171–177. https://doi.org/10.1007/S10853-005-5703-4/METRICS
93. Liu G, Zhou B, Ni X et al. (2012) Influence of thermal process on microstructural and physical properties of ambient pressure dried hydrophobic silica aerogel monoliths. J Sol-Gel Sci Technol 62:126–133. https://doi.org/10.1007/s10971-012-2694-x
94. Udvardi, Kovács IJ B, Fancsik T et al. (2017) Effects of Particle Size on the Attenuated Total Reflection Spectrum of Minerals. Appl Spectrosc 71:1157–1168. https://doi.org/10.1177/0003702816670914/ASSET/IMAGES/LARGE/10.1177_0003702816670914-FIG6.JPEG
95. Akhter F, Jamali AR, Khan W (2023) TEOS-Doped vs Non-TEOS Silica Aerogels: a Comparative Study of Synthesis, Characterization, Isotherm Studies and Performance Evaluation for Pb (II) Removal from Synthetic Wastewater. Water Air Soil Pollut 234:1–9. https://doi.org/10.1007/S11270-022-06051-4/TABLES/3
96. Shao Z, Luo F, Cheng X, Zhang Y (2013) Superhydrophobic sodium silicate based silica aerogel prepared by ambient pressure drying. Mater Chem Phys 141:570–575. https://doi.org/10.1016/J.MATCHEMPHYS.2013.05.064
97. Florensa M, Llenas M, Medina-Gutiérrez E et al.(2022) Key Parameters for the Rational Design, Synthesis, and Functionalization of Biocompatible Mesoporous Silica Nanoparticles Pharmacology 14:2703. https://doi.org/10.3390/PHARMACEUTICS14122703
98. Tadjarodi A, Mohammadi V, Haghverdi M (2012) Preparation and characterization of nano-porous silica aerogel from rice husk ash by drying at atmospheric pressure. Mater Res Bull 47:2584–2589. https://doi.org/10.1016/j.materresbull.2012.04.143
99. Biglari Quchan Atigh Z, Heidari A, Karimi A et al. (2021) Purification and economic analysis of nanoclay from bentonite. Environ Sci Pollut Res 28:13690–13696. https://doi.org/10.1007/S11356-020-11595-1/TABLES/4
100. Andrunik M, Bajda T(2019) (2019) Modification of Bentonite with Cationic and Nonionic Surfactants: Structural and Textural Features. Materials 12:3772. https://doi.org/10.3390/MA12223772
101. Manuale DL, Greco E, Clementz A et al. (2014) Biodiesel purification in one single stage using silica as adsorbent. Chem Eng J 256:372–379. https://doi.org/10.1016/J.CEJ.2014.07.022
102. Kamath SR, Proctor A (1998) Silica Gel from Rice Hull Ash: Preparation and Characterization. Cereal Chem 75:484–487. https://doi.org/10.1094/CCHEM.1998.75.4.484
103. White RJ, Budarin V, Luque R et al. (2009) Tuneable porous carbonaceous materials from renewable resources. Chem Soc Rev 38:3401–3418. https://doi.org/10.1039/B822668G
104. Erkan H, Keçeciler-Emir C, Özel C, Yücel S (2023) Posaconazole Loading and Release Behavior in Surface-Modified Mesoporous Silica Nanoparticular System. Erzincan Univ J Sci Technol 16:615–632. https://doi.org/10.18185/ERZIFBED.1189339
105. Barakan S, Aghazadeh V, Samiee Beyragh A, Mohammadi S (2020) Thermodynamic, kinetic and equilibrium isotherm studies of As(V) adsorption by Fe(III)-impregnated bentonite. Environ Dev Sustain 22:5273–5295. https://doi.org/10.1007/S10668-019-00424-2/FIGURES/11
106. Thommes M, Kaneko K, Neimark AV et al. (2015) Physisorption of gases, with special reference to the evaluation of surface area and pore size distribution (IUPAC Technical Report). Pure Appl Chem 87:1051–1069. https://doi.org/10.1515/pac-2014-1117
107. Chen Q, Wang H, Sun L (2017) Preparation and Characterization of Silica Aerogel Microspheres. Materials (Basel) 10:435. https://doi.org/10.3390/ma10040435
108. Balci S, Gökçay E (2009) Pore structure and surface acidity evaluation of Fe-PILCs. Turkish J Chem 33:843–856. https://doi.org/10.3906/kim-0807-17
109. Yuliana M, Ismadji S, Lie J et al. (2022) Low-cost structured alginate-immobilized bentonite beads designed for an effective removal of persistent antibiotics from aqueous solution. Environ Res 207:112162. https://doi.org/10.1016/J.ENVRES.2021.112162
110. Nde-Aga BJ, Kamga R, Nguetnkam JP (2007) Adsorption of palm oil carotene and free fatty acids onto acid activated cameroonian clays. J Appl Sci 7:2462–2467. https://doi.org/10.3923/JAS.2007.2462.2467
111. Maddikeri GL, Pandit AB, Gogate PR (2012) Adsorptive removal of saturated and unsaturated fatty acids using ion-exchange resins. Ind Eng Chem Res 51:6869–6876. https://doi.org/10.1021/IE3000562/ASSET/IMAGES/LARGE/IE-2012-000562_0008.JPEG

112. Mag TK (1990) Bleaching-theory and practice. In: Proceedings of the Edible Fats and Oils Processing World Conference. American Oil Chemists' Society Champaign, pp 107–116
113. Jean Baptiste BM, Daniele BK, Marie Charlène E et al. (2020) Adsorption mechanisms of pigments and free fatty acids in the discoloration of shea butter and palm oil by an acid-activated Cameroonian smectite. Sci African 9:e00498. https://doi.org/10.1016/J.SCIAF.2020.E00498
114. Sobrinho RAL, Andrade GRS, Costa LP et al. (2019) Ordered micro-mesoporous carbon from palm oil cooking waste via nanocasting in HZSM-5/SBA-15 composite: Preparation and adsorption studies. J Hazard Mater 362:53–61. https://doi.org/10.1016/J.JHAZMAT.2018.08.097
115. Nuru Z, Getachew P (2021) Improving the quality of used frying niger seed oil with adsorbent treatment. Heliyon 7:e06748. https://doi.org/10.1016/J.HELIYON.2021.E06748
116. Boki K, Kubo M, Wada T, Tamura T (1992) Bleaching of alkali-refined vegetable oils with clay minerals. J Am Oil Chem Soc 69:232–236. https://doi.org/10.1007/BF02635892/METRICS
117. Adhikari C, Proctor A, Blyholder GD (1997) An infrared spectroscopy study of lipid adsorption from hexane onto an acid-activated bleaching clay. JAOCS. J Am Oil Chem Soc 74:1265–1268. https://doi.org/10.1007/S11746-997-0055-7/METRICS
118. Gil B, Kim M, Kim JH, Yoon SH (2014) Comparative study of soybean oil refining using rice hull silicate and commercial adsorbents. Food Sci Biotechnol 23:1025–1028
119. Kalapathy U, Proctor A (2000) New method for free fatty acid reduction in frying oil using silicate films produced from rice hull ash. JAOCS. J Am Oil Chem Soc 77:593–598. https://doi.org/10.1007/S11746-000-0095-4/METRICS
120. Hamm W, Hamilton RJ, Calliauw G (2013) Edible oil processing. Wiley Online Library
121. O'Brien RD (2008) Fats and Oils: Formulating and Processing for Applications, Third Edition, Third edition. CRC Press
122. Erickson DR (1990) Edible fats and oils processing: basic principles and modern practices: World Conference Proceedings. The American Oil Chemists Society
123. Susilowati S, Astya KL, Bachri US (2021) Reducing Peroxide Value In Used Cooking Oil Using Ampo As An Adsorbent. Int J Eco-Innovation Sci Eng 2:1–8. https://doi.org/10.4186/ijeise.upnjatim.ac.id/
124. AOCS (1998) Oil Purification. In: Bockisch M (ed) Fats and Oils Handbook. AOCS Press, pp 613–718
125. Toeneboehn GJ, Welsh WA, Iii WMC, Bogdanor JM (1992) Modified physical refining process for treating glyceride oils, fatty chemicals and wax esters
126. Farag RS, Basuny AMM (2009) Improvement in the quality of used sunflower oil by organic and inorganic adsorbents. Int J Food Sci Technol 44:1802–1808. https://doi.org/10.1111/J.1365-2621.2009.02002.X
127. Mumtaz F, Zubair M, Khan F, Niaz K (2020) Analysis of plants lipids. Recent Adv Nat Prod Anal 677–705. https://doi.org/10.1016/B978-0-12-816455-6.00022-6
128. Mota MFS, Waktola HD, Nolvachai Y, Marriott PJ (2021) Gas chromatography – mass spectrometry for characterisation, assessment of quality and authentication of seed and vegetable oils. TrAC Trends Anal Chem 138:116238. https://doi.org/10.1016/J.TRAC.2021.116238
129. Romanić R (2020) Cold pressed sunflower (Helianthus annuus L.) oil. Cold Press Oils Green Technol Bioact Compd Funct Appl 197–218. https://doi.org/10.1016/B978-0-12-818188-1.00017-7
130. Carelli AA, Brevedan MIV, Crapiste CH (1997) Quantitative determination of phospholipids in sunflower oil. J Am Oil Chem Soc 74:511–514. https://doi.org/10.1007/S11746-997-0173-2
131. Ali AH, Zou X, Abed SM et al. (2019) Natural phospholipids: Occurrence, biosynthesis, separation, identification, and beneficial health aspects. Crit Rev Food Sci Nutr 59:253–275. https://doi.org/10.1080/10408398.2017.1363714
132. Foodelphi.com (2020) Yağ Rafinasyonu ve Yağların Raf Ömrü / Oil Refining and Shelf Life of Oils. https://www.foodelphi.com/yag-rafinasyonu-ve-yaglarin-raf-omru/. Accessed 19 Dec 2023
133. Shihab JM, Rashid KT, Toma MA (2022) A review on membrane technology application for vegetable oil purification processes. Int J Food Eng 18:655–677. https://doi.org/10.1515/IJFE-2022-0058/MACHINEREADABLECITATION/RIS
134. Salam MA, Creaser D, Arora P et al.(2018) Influence of Bio-Oil Phospholipid on the Hydrodeoxygenation Activity of NiMoS/Al2O3 Catalyst Catalyst 8:418. https://doi.org/10.3390/CATAL8100418
135. Ghazani SM, García-Llatas G, Marangoni AG (2013) Minor constituents in canola oil processed by traditional and minimal refining methods. JAOCS, J Am Oil Chem Soc 90:743–756. https://doi.org/10.1007/S11746-013-2215-2/METRICS
136. Havlik P, Abhari R, Roth G, Tomlinson HL (2013) Method for the removal of phosphorus
137. Van Dalen JP, Brunia L (1991) Process for refining glyceride oil using silica hydrogel
138. Chen X, Sun S(2023) Color Reversion of Refined Vegetable Oils: A Review Molecules 28:5177. https://doi.org/10.3390/MOLECULES28135177
139. Zhang K, Van Dyk L, He D et al. (2021) Synthesis of zeolite from fly ash and its adsorption of phosphorus in wastewater. Green Process Synth 10:349–360. 10.1515/GPS-2021-0032/ASSET/GRAPHIC/J_GPS-2021-0032_FIG_008.JPG
140. Liu W (2001) Modeling description and spectroscopic evidence of surface acid–base properties of natural illites. Water Res 35:4111–4125. https://doi.org/10.1016/S0043-1354(01)00156-7
141. Proctor A, Harris CD (1996) Soy hull carbon as an adsorbent of minor crude soy oil components. JAOCS. J Am Oil Chem Soc 73:527–529. https://doi.org/10.1007/BF02523931/METRICS
142. Gnanasambandam R, Proctor A (1997) Soy hull as an adsorbent source in processing soy oil. JAOCS. J Am Oil Chem Soc 74:685–692. https://doi.org/10.1007/S11746-997-0201-2/METRICS
143. Vaisali C, Charanyaa S, Belur PD, Regupathi I (2015) Refining of edible oils: A critical appraisal of current and potential technologies. Int J Food Sci Technol 50:13–23. https://doi.org/10.1111/IJFS.12657
144. Ghazani SM, Marangoni AG (2013) Minor components in canola oil and effects of refining on these constituents: A review. J Am Oil Chem Soc 90:923–932. https://doi.org/10.1007/S11746-013-2254-8/METRICS
145. García-Moreno PJ, Guadix A, Gomez-Robledo L et al. (2013) Optimization of bleaching conditions for sardine oil. J Food Eng 116:606–612. https://doi.org/10.1016/J.JFOODENG.2012.12.040
146. Al-Zahrani AA, Al-Shahiani SS, Al-Tawil YA (2001) Study on the Activation of Saudi Natural Bentonite, Part II: Characterization of the Produced Active Clay and Its Test as an Adsorbing Agent. J King Saud Univ - Eng Sci 13:193–202. https://doi.org/10.1016/S1018-3639(18)30733-5
147. Khan S, Ajmal S, Hussain T et al. (2023) Clay-based materials for enhanced water treatment: adsorption mechanisms, challenges, and future directions J Umm Al-Qura Univ Appl Sci (1):1–16. 10.1007/S43994-023-00083-0
148. Sun B, Gao P, Yu H et al. (2023) Optimization of Composite Decolorizer Efficacy Based on Decolorization Efficiency,

Toxicity, and Nutritional Value of Rice Bran Oil. J Oleo Sci 72:755–765. https://doi.org/10.5650/JOS.ESS23050
149. Sabah E, Çelik MS (2005) Sepiolite: An effective bleaching adsorbent for the physical refining of degummed rapeseed oil. J Am Oil Chem Soc 82:911–916. https://doi.org/10.1007/S11746-005-1164-4
150. Su D, Xiao T, Gu D et al. (2013) Ultrasonic bleaching of rapeseed oil: Effects of bleaching conditions and underlying mechanisms. J Food Eng 117:8–13. https://doi.org/10.1016/J.JFOODENG.2013.01.039
151. Parekh K, Shahabuddin S, Gaur R, Dave N (2022) Prospects of conducting polymer as an adsorbent for used lubricant oil reclamation. Mater Today Proc 62:7053–7056. https://doi.org/10.1016/J.MATPR.2022.01.130
152. Hu Y, Ma C, Huang W et al. (2023) Adsorption behavior of activated carbon for the elimination of zearalenone during bleaching process of corn oil. Grain Oil Sci Technol 6:24–33. https://doi.org/10.1016/J.GAOST.2022.11.002
153. Brooks DD, Berbesi R, Hodgson AS (2019) Optimization of bleaching process. AOCS lipid Libr
154. Taylor DR, Jenkins DB (1988) Acid-activated clays. Soc Min Eng AIME Trans 282:1901–1910
155. Siew WL, Tan YA, Tang TS (1994) Silica refining of palm oil. J Am Oil Chem Soc 71:1013–1016. https://doi.org/10.1007/BF02542271/METRICS
156. Yao Y, Liu C, Xiong W et al. (2020) Silicon dioxide as an efficient adsorbent in the degumming of rapeseed oil. J Clean Prod 268:122344. https://doi.org/10.1016/J.JCLEPRO.2020.122344
157. Huang J, Liu Y, Liu Y, Wang X (2007) Effect of attapulgite pore size distribution on soybean oil bleaching. JAOCS. J Am Oil Chem Soc 84:687–692. https://doi.org/10.1007/S11746-007-1094-9/FIGURES/4
158. Eskin M, Nag A (2010) Extraction, Refining, and Stabilization of Edible Oils. In: Nag A (ed) Biosystems Engineering, 1st Editio. McGraw-Hill Education, New York
159. Zhou L, Shen J, Tse TJ et al. (2022) Electrostatic field treatment as a novel and efficient method for refining crude canola oil. J Clean Prod 360:131905. https://doi.org/10.1016/J.JCLEPRO.2022.131905
160. Cheryan M (2005) Membrane technology in the vegetable oil industry. Membr Technol 5–7. 10.1016/S0958-2118(05)70387-6
161. Yates RA, Caldwell JD (1992) Adsorptive capacity of active filter aids for used cooking oil. J Am Oil Chem Soc 69:894–897. https://doi.org/10.1007/BF02636340/METRICS
162. Dimic E, Karlovic D, Turkulov J (1994) Pretreatment efficiency for physical refining of sunflower seed oil. J Am Oil Chem Soc 71:1357–1361. https://doi.org/10.1007/BF02541355/METRICS
163. Proctor A, Clark PK, Parker CA (1995) Rice hull ash adsorbent performance under commercial soy oil bleaching conditions. J Am Oil Chem Soc 72:459–462. https://doi.org/10.1007/BF02636089/METRICS
164. Maskan M, Bağci HI (2003) Effect of different adsorbents on purification of used sunflower seed oil utilized for frying. Eur Food Res Technol 217:215–218. https://doi.org/10.1007/S00217-003-0731-2/TABLES/5
165. Wang X, Wang T, Johnson LA (2002) Composition and sensory qualities of minimum-refined soybean oils. JAOCS. J Am Oil Chem Soc 79:1207–1214. https://doi.org/10.1007/S11746-002-0629-9/METRICS
166. Ismail SAEA, Ali RFM (2015) Physico-chemical properties of biodiesel manufactured from waste frying oil using domestic adsorbents. Sci Technol Adv Mater 16:. https://doi.org/10.1088/1468-6996/16/3/034602
167. Wang T, Johnson LA (2001) Natural refining of extruded-expelled soybean oils having various fatty acid compositions. JAOCS. J Am Oil Chem Soc 78:461–466. https://doi.org/10.1007/S11746-001-0286-Z/METRICS
168. Chang YY, Lin CI, Chen HK (2001) Rice hull ash structure and bleaching performance produced by ashing at various times and temperatures. JAOCS. J Am Oil Chem Soc 78:657–660. https://doi.org/10.1007/S11746-001-0322-Z/METRICS
169. Kim M, Yoon SH, Choi E, Gil B (2008) Comparison of the adsorbent performance between rice hull ash and rice hull silica gel according to their structural differences. LWT - Food Sci Technol 41:701–706. https://doi.org/10.1016/J.LWT.2007.04.006
170. Yilmaz E, Deviren A (2022) Silica gel 60 removes bitterness from cold-press produced grapefruit seed oil by adsorption principle. Flavour Fragr J 37:52–62. https://doi.org/10.1002/FFJ.3683
171. Ayu Putranti MLT, Wirawan SK, Bendiyasa IM (2018) Adsorption of Free Fatty Acid (FFA) in Low-Grade Cooking Oil Used Activated Natural Zeolite as Adsorbent. IOP Conf Ser Mater Sci Eng 299:012085. https://doi.org/10.1088/1757-899X/299/1/012085
172. Tandewi SAMS, Hambali E (2022) Refining of Fish Oil from Fish Meal Processing By-product Using Zeolite and Bleaching Earth. IOP Conf Ser Earth Environ Sci 1034:012050. https://doi.org/10.1088/1755-1315/1034/1/012050